

Review Article

Open Access



Vacuum filtration method towards flexible thermoelectric films

Chenxi Wang¹, Qing Liu¹, Haijun Song^{1,*}, Qinglin Jiang^{2*}

¹College of Information Science and Engineering, Jiaxing University, Jiaxing 314001, Zhejiang, China.

²State Key Laboratory of Luminescent Materials and Devices, South China University of Technology, Guangzhou 510640, Guangdong, China.

*Correspondence to: Dr. Haijun Song, College of Information Science and Engineering, Jiaxing University, 899 Guangqiong Road, Nanhu District, Jiaxing 314001, Zhejiang, China. E-mail: songhaijun8837@126.com; Prof. Qinglin Jiang, State Key Laboratory of Luminescent Materials and Devices, South China University of Technology, 381 Wu-shan Road, Tianhe District, Guangzhou 510640, Guangdong, China. E-mail: jiangql@scut.edu.cn

How to cite this article: Wang C, Liu Q, Song H, Jiang Q. Vacuum filtration method towards flexible thermoelectric films. *Soft Sci* 2023;3:34. <https://dx.doi.org/10.20517/ss.2023.25>

Received: 31 May 2023 **First Decision:** 21 Jun 2023 **Revised:** 20 Jul 2023 **Accepted:** 31 Jul 2023 **Published:** 10 Oct 2023

Academic Editor: Zhifeng Ren **Copy Editor:** Dong-Li Li **Production Editor:** Dong-Li Li

Abstract

Thermoelectric (TE) conversion technology can directly exploit the temperature difference of several Kelvin between the human body and the environment to generate electricity, which provides a self-powered solution for wearable electronics. Flexible TE materials are increasingly being developed through various methods, among which the vacuum filtration method stands out for its unique advantages, attracting the favor of researchers. It has been proven to construct flexible TE thin films with excellent performance effectively. This paper presents a comprehensive overview and survey of the advances of the vacuum filtration method in producing flexible TE thin films. The materials covered in this study include conducting polymer-based materials, carbon nanoparticle-based materials, inorganic materials, two-dimensional materials, and ternary composites. Finally, we explore potential research outlooks and the significance of flexible films, which are at the forefront of research in TE materials science.

Keywords: Thermoelectric, vacuum filtration, flexible film

INTRODUCTION

As humans enter the Internet of Things era, autonomous sensors play essential roles in various fields, such as biometric monitoring, medical monitoring, and industrial and environmental controls. Moreover, there



© The Author(s) 2023. **Open Access** This article is licensed under a Creative Commons Attribution 4.0 International License (<https://creativecommons.org/licenses/by/4.0/>), which permits unrestricted use, sharing, adaptation, distribution and reproduction in any medium or format, for any purpose, even commercially, as long as you give appropriate credit to the original author(s) and the source, provide a link to the Creative Commons license, and indicate if changes were made.



is an unprecedented demand for portable, reliable, ultra-thin, and sustainable wearable electronic power devices. The application of conventional batteries is limited because of their frequent replacement/recharge and extra maintenance. Therefore, developing a maintenance-free and self-powered sensor system is critically important. Thermoelectric (TE) conversion technology can convert heat from the body or the environment into electricity, providing a viable self-powered solution for flexible electronics^[1-3]. Conventional inorganic bulk TE materials, such as Bi₂Ti₃ and PbTe, usually show high TE performance; however, brittle and rigid properties of inorganic materials and the complicated process have limited their applicability, particularly when in contact with curved or irregular heat sources^[4,5]. In this situation, film-based flexible TE materials and generators show significant advantages and application prospects since their conformability enables effective contact with all kinds of curved or irregular heat sources to maximize heat harvesting. Besides, a thin-film thermoelectric generator (TEG) may use fewer materials compared to a bulk TEG and provide easy integration with integrated circuits^[6,7]. **Figure 1** shows the different structures of traditional inorganic TEGs with a cross-plane structure in **Figure 1A** and thin-film TEGs with an in-plane structure in **Figure 1B**. Traditional inorganic TEGs are composed of bulk P/N legs tiled in two dimensions over a ceramic substrate patterned with electrical contacts, in which the temperature gradient across the material is perpendicular to the substrate. Unlike cross-plane structures, the temperature gradient across the material is parallel to the substrate for the in-plane structure. In this structure, the temperature gradient across the TE legs is usually minimal; creative strategies, such as corrugated, origami, and rolled designs^[8,9], can convert the 2D arrays of thin-film TE legs into 3D architectures. Thus, the temperature gradient will parallel the substrate to obtain a more significant thermal gradient. A flexible TEG has the advantages of all-weather continuous operation, no moving parts, small size, and high reliability. Developing high-performance, low-cost, and easy-to-process materials is the pursuit of the TE field. The properties are measured primarily by the dimensionless TE value (ZT): $ZT = \sigma S^2 T / \kappa$. High-performance TE materials require high electrical conductivity σ , a high Seebeck coefficient S , and low thermal conductivity κ .

Research on flexible TE technology generally consists of two strategies. One is to directly use organic TE materials with good flexibility and plasticity, and the other is to integrate brittle inorganic TE materials into the flexible substrate.^[10-13] The former has lower electrical performance, resulting in output voltage and power much inferior to inorganic materials; the latter is difficult to produce ultra-thin flexible devices due to its complex structure and technology. The discovery of silver sulfide-based ductile semiconductors has extensively promoted the development of flexible inorganic TE materials^[14-16]. Significantly, Yang *et al.* reported high-performance p-type ductile TE materials of AgCu(S_xSe_{1-x}) pseudo ternary solid solutions, with a ZT value of 0.45 at 300 K^[14]. They developed ultra-thin flexible TE devices with a conventional π -shape and demonstrated ultra-high normalized power density and reasonable service stability. On the other hand, organic TE materials, while fully leveraging their advantages of flexibility, solution-processable, and low intrinsic thermal conductivity, have been steadily addressing their limitations in common overall TE properties and have achieved rapid development over the past decade, with ZT values of multiple material systems exceeding 0.1 at room temperature, constantly expanding the application range of wearable devices^[17-20].

The preparation process of flexible TE films is crucial in constructing wearable TE devices. Inorganic plastic semiconductors are prepared first by traditional melting and annealing methods, and then the prepared inorganic material is cut into thin sheets. In addition, Jin *et al.* prepared high-performance Bi₂Te₃-single-walled carbon nanotube (SWCNT) composite flexible self-supported TE thin films with carbon nanotubes (CNTs) as the skeleton using independently improved magnetron sputtering deposition equipment^[21]. Vacuum filtration^[22-24], vapor deposition^[25-28], printing^[29-31], and coating^[32-34] methods effectively prepare

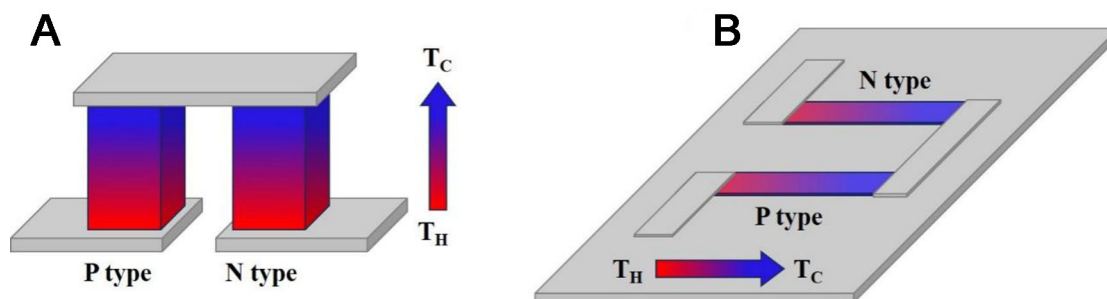


Figure 1. Schematic diagram of traditional inorganic TEGs with a cross-plane structure (A) and thin-film TEGs (B) with an in-plane structure (T_H , hot-side temperature, T_C , cool-side temperature). TEG: Thermoelectric generator.

flexible TE films, utilizing substrates such as polyvinylidene fluoride (PVDF), cotton, polyimide, *etc.* Compared with other preparation methods, vacuum filtration is simple, effective, and economical. The detailed process includes the following steps: (1) connection of filter flask to a vacuum pump; (2) installation of filter papers; (3) pouring of solution; (4) vacuum filtration of solution; (5) the drying process. The materials of filter papers are various, including polytetrafluoroethylene (PTFE), PVDF, polyethersulfone (PES), polypropylene (PP), nylon, cellulose acetate (CA), *etc.* Moreover, they can be classified as organic and water series according to the materials. During vacuum filtration, users may choose the proper filter papers according to the different solutions. The size of filter papers ranges from 13 to 25 to 500 mm, and they should be chosen to match the size of the filter flask. The pore size of the filter papers ranges from 0.2, 0.22, 0.45, and 1.0 μm to tens of microns. Carbon nanomaterials, inorganic nanoparticles, PTFE, PVDF, nylon, and CA-based filter papers with sizes of 0.2 and 0.22 μm are mainly used to prevent the loss of nano components in the solution. Besides, the vacuum filtration method has some other unique advantages: (1) It can use the pressure difference, combined with the subsequent cold/hot pressing process, to compress the material very tightly to obtain the compact, flexible film. This is especially beneficial for some composite TE materials, which are challenging to achieve in the drip coating or spin coating processes; (2) Some impurities or non-conductive groups, such as poly(4-styrenesulfonic acid) (PSS) in poly(3,4-ethylenedioxythiophene) (PEDOT):PSS, will affect the TE performance, but they can be removed through filtration to achieve excellent performance.

Unlike the recently published reviews on flexible TE materials, this paper focuses on the research progress of vacuum filtration for preparing flexible TE films. The structure of this review is outlined in Figure 2. The advantages and a range of representative examples of the vacuum filtration method in producing flexible TE thin films, including conducting polymer-based, carbon nanoparticle-based, inorganic, two-dimensional materials, and ternary composites, will be discussed. Furthermore, the present challenges and future development opportunities of this method are forecasted. Given the effectiveness of this method and its broad relevance to other fields of research, we will do our best to guide interested readers to this field, which can be applied and promoted to new heights in the future.

CONDUCTING POLYMER-BASED TE MATERIALS

PEDOT-based TE materials

Polymer semiconductors, as TE materials, offer unique advantages, such as high electrical conductivity, low inherent thermal conductivity, cost-effectiveness, mass production using simple synthesis methods, and the ability to deposit over large areas. Especially, PEDOT, which forms a complex with PSS, is considered the most promising conductive polymer for TE. Previously, PEDOT:PSS TE thin films were prepared mainly based on drip or spin coating on a glass substrate. Considering the future need for large-scale preparation

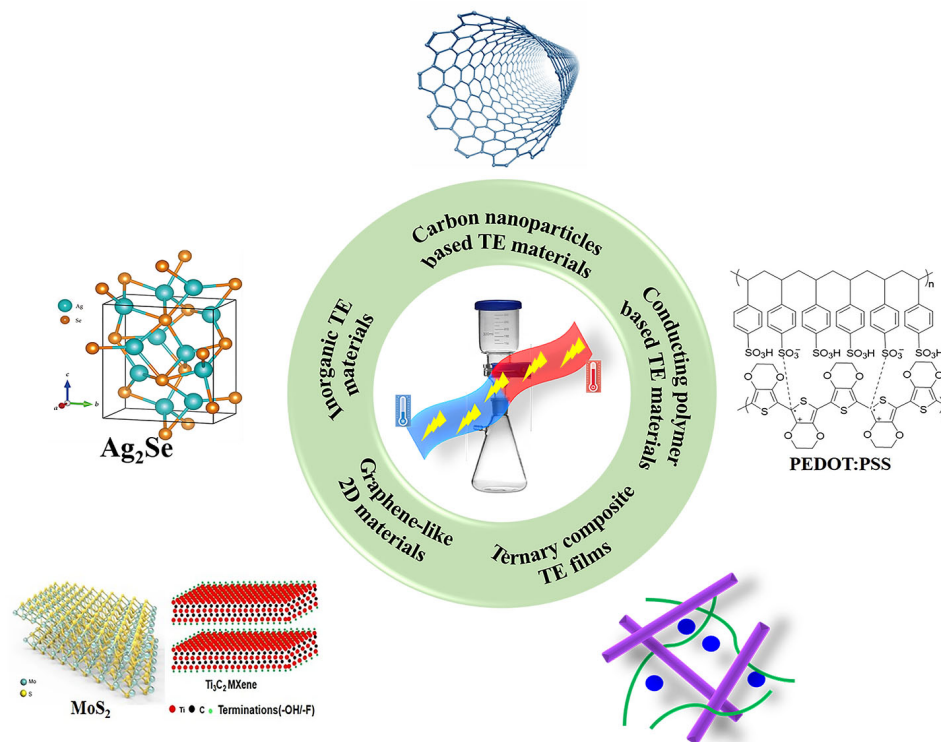


Figure 2. Schematic outline of this review. PEDOT:PSS: Poly(3,4-ethylenedioxythiophene):poly(4-styrenesulfonic acid); TE: thermoelectric.

and flexible wearable applications, it is necessary to develop new preparation methods to obtain large-size flexible thin films. In 2015, Mengistie *et al.* prepared free-standing, flexible smooth PEDOT:PSS bulky papers through vacuum-assisted filtration^[23] [Figure 3A]. In vacuum filtration, the liquid is sucked into the filtration membrane by the pump, resulting in a higher filtration rate than gravity filtration. After vacuum drying, the bulky paper can easily peel off the Anodisc filter membrane.

Apart from being a counterion, PSS is also used as a charge compensator and template for the polymerization of PEDOT in PEDOT:PSS, making it readily dispersible in water. Two PSS types are present in PEDOT:PSS solutions: “main PSS” (complexed to PEDOT grains) and “free PSS” (act as surfactants to reduce intermolecular interactions between two PEDOT grains). However, in excess, PSS is an insulator (non-ionizing dopant), which is the main reason for the low conductivity of commercial PEDOT. Selective removal of PSS is one of the mechanisms to improve electrical conductivity. Numerous approaches have been reported for enhancing the TE performance of PEDOT:PSS, such as post-treatment methods based on doping and de-doping, including overcoating, dipping, or vapor-treatment ways, which may affect the oxidation level and electron transport properties that are strongly associated with TE performance.

In the above experiment by Mengistie *et al.*, they used methanol, formic acid (FA), ethylene glycol (EG), and polyethylene glycol (PEG) to treat PEDOT:PSS, respectively^[23]. EG and PEG200 were mixed with PEDOT:PSS before being filtered under pressure. The difference lies in the treatment of annealed bulky papers, which were treated with methanol and FA. Surface PSS was relatively reduced as excess PSS was flushed away by methanol and FA treatment [Figure 3B]. For EG- and PEG-treated papers, no PSS is removed from the surface. Instead, the PSS layer is depleted from the surface, which becomes rich in

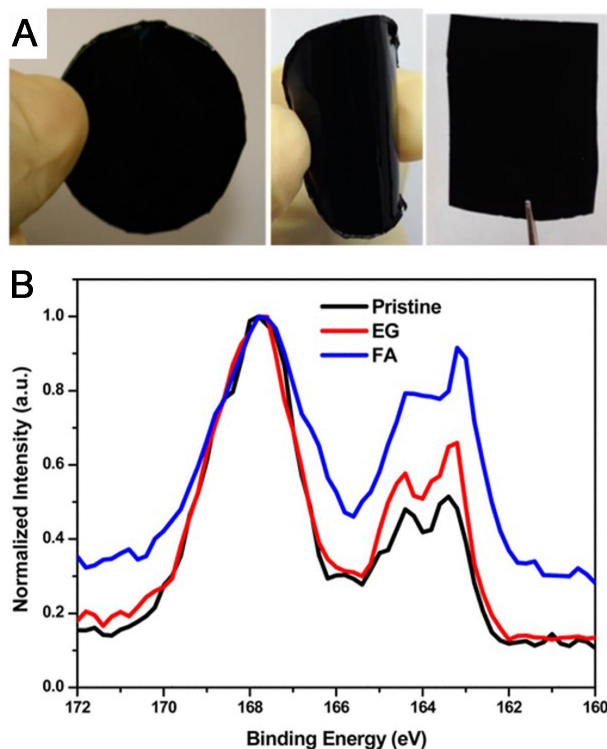


Figure 3. (A) Photos of Flexible PEDOT:PSS bulky papers; (B) S(2p) XPS spectra of PEDOT:PSS bulky papers: pristine, treated with EG, and treated with FA. Reproduced with permission from Ref.^[23]. Copyright © 2015. American Chemical Society. EG: Ethylene glycol; PEDOT:PSS: poly(3,4-ethylenedioxythiophene):poly(4-styrenesulfonic acid).

PEDOT. The amount of PSS removed/exhausted from the PEDOT:PSS paper is consistent with the respective conductivity enhancement. The average conductivities of EG-, PEG-, methanol-, and FA-treated papers are 640, 800, 1,300, and 1,900 S/cm, respectively. Removing PSS, especially from the final film, is essential for improving electrical conductivity.

The current post-treatment technology has low practicability due to various problems, including difficulty in mass production, lengthy and complicated processes, swelling and falling of polymers on the film surface during the dipping process, *etc.* To solve this problem, Lee *et al.* reported a solution treatment method using ultrafiltration to remove excess PSS molecules directly from PEDOT:PSS dispersions without post-treatment^[35]. The impurities, such as PSS, EDOT oligomers in solution, residual oxidants, and excess electrolytes, were all smaller than the membrane pore size. Consequently, they are flushed out of the cell through the membrane by distilled deionized water. Moreover, the water is continuously filled into the ultrafiltration cell to maintain a stable concentration of the suspended PEDOT:PSS in the feed solution. In ultrafiltration, the suspension of PEDOT:PSS will be kept on the membrane because the solute is larger than the membrane pore size (100 nm). On the other hand, hydrazine is used as a chemical dedopant because it can decrease the oxidation level to improve the Seebeck coefficient. De-doped PEDOT:PSS was prepared by adding excess hydrazine into the PEDOT:PSS solution. The hydrazine molecules that are not incorporated into the main PSS are removed along with free PSS during ultrafiltration. Finally, the two PEDOT:PSS solutions were mixed in different ratios by simple ultrasonication blending, and the *ZT* value of 0.2 was recorded. These results show that filtration is an effective way to remove PSS, but unfortunately, the final film formation method is a spin coating on the glass substrate.

Furthermore, Xiong *et al.* developed one-step direct dilution to achieve stable, simple, and fast integration of PEDOT:PSS film preparation and solvent treatment^[36]. Due to the PSS partly dissolved in the organic solvent, the dilution process caused by PSS initially scattered away from the PEDOT-rich nanoparticle aggregation significantly. The PEDOT:PSS film on PVDF was thin and flexible, so researchers could cut it into any desired form and paste it onto a transparent PET substratum. This approach is expected to affect the electrical and TE properties positively because it avoids the waste of pristine PEDOT:PSS, the limitation of solvent types, the use of sophisticated instruments, and complex processes. The obtained PEDOT:PSS thin films have high electrical conductivity of about 1,500 S/cm and a considerable ZT value of 0.1 with facile treatment for the high or low-boiling-point solvents.

Previous works mainly used commercial PEDOT:PSS to prepare free-standing PEDOT-based films. However, compared with the EDOT monomer, the cost of commercial PEDOT:PSS is too high, which is unsuitable for application in the TE field. Song *et al.* filtered and obtained a flexible, independent PEDOT nanofiber film through a simple self-assembled micellar soft template method [Figure 4A-D]^[37]. The processing method perfectly solves the problem that PEDOT is difficult to handle due to its insoluble and refractory properties. By incorporating SWCNTs into PEDOT nanofibers, the PEDOT nanofiber/SWCNTs showed a power factor of 14.4 $\mu\text{W}/\text{mK}^2$. Ni *et al.* successfully used a modified self-assembled micellar soft-template method and vacuum-assisted filtration to prepare flexible free-standing and high-conductive (1,340 S/cm) PEDOT nanowire (NW) film^[38]. The film was treated with acid and base to further optimize the TE properties. The power factor of the best PEDOT NW film was 46.51 $\mu\text{W}/\text{mK}^2$. Finally, a flexible TEG assembled on polyimide consisting of six optimum PEDOT NW thin-film-silver thermocouples was obtained to demonstrate TE power generation [Figure 4E and F].

PEDOT/inorganic composite TE materials

Despite the high electrical conductivity of PEDOT, its low Seebeck coefficient, typically ranging from 15 to 20 $\mu\text{V}/\text{K}$ ^[10,39,40], has become the main obstructive factor for its TE performance. Incorporating inorganic semiconductors with a high Seebeck coefficient or power factor into PEDOT seems to be a good strategy, which can fully use the advantages of PEDOT and inorganic components. Furthermore, PEDOT-based composite films with high quality can be obtained by dispersing inorganic materials into PEDOT:PSS solution, followed by a simple and effective vacuum filtration method.

Inorganic semiconductor materials, such as Te-, CuSe-, Bi-Te-based alloys, *etc.*, are usually the first choice to construct PEDOT-based composites. Song *et al.* have conducted excellent work in this field. In 2017, they prepared PEDOT:PSS-functionalized Te (PF-Te) nanorods. The PEDOT:PSS layer provided excellent dispersibility in the PEDOT:PSS solution, and then PEDOT:PSS/PF-Te composite films were obtained through a vacuum filtration method using a 0.22 μm PVDF porous membrane [Figure 5]^[41]. Because of the high Seebeck coefficient of Te nanorods and an energy filtering effect between the PEDOT:PSS layer and Te, the Seebeck coefficient of the composites was enhanced from 15.6 to 51.6 $\mu\text{V}/\text{K}$. The highest power factor reached 51.4 $\mu\text{W}/\text{mK}^2$ for the sample containing 70 wt% PF-Te nanorods. Also, flexible PEDOT:PSS/Ag₂Te nanocomposite films on the PES substrate were prepared through vacuum filtration and cold pressing processes using PF-Te nanorods as the templates^[42]. An optimal PEDOT:PSS/Ag₂Te nanocomposite film exhibited a power factor of 143.3 $\mu\text{W}/\text{mK}^2$ at room temperature. In 2019, they prepared PEDOT:PSS-coated Cu_xSe_y (PC-Cu_xSe_y) NWs through a wet-chemical method, and then they fabricated PEDOT:PSS/Cu_xSe_y nanocomposite films on flexible nylon membranes by vacuum filtration and cold-press processes [Figure 6]^[43]. When the Cu/Se nominal molar ratio is three, the composite showed the highest power factor of ~ 270.3 $\mu\text{W}/\text{mK}^2$ at 300 K. Additionally, due to the nanoporous structure of a composite film, the intrinsic flexibility of nylon and the good combination between nylon and film, the composite film showed excellent flexibility. In another study, hot pressing at 200 °C and 1 MPa was employed to replace cold pressing to

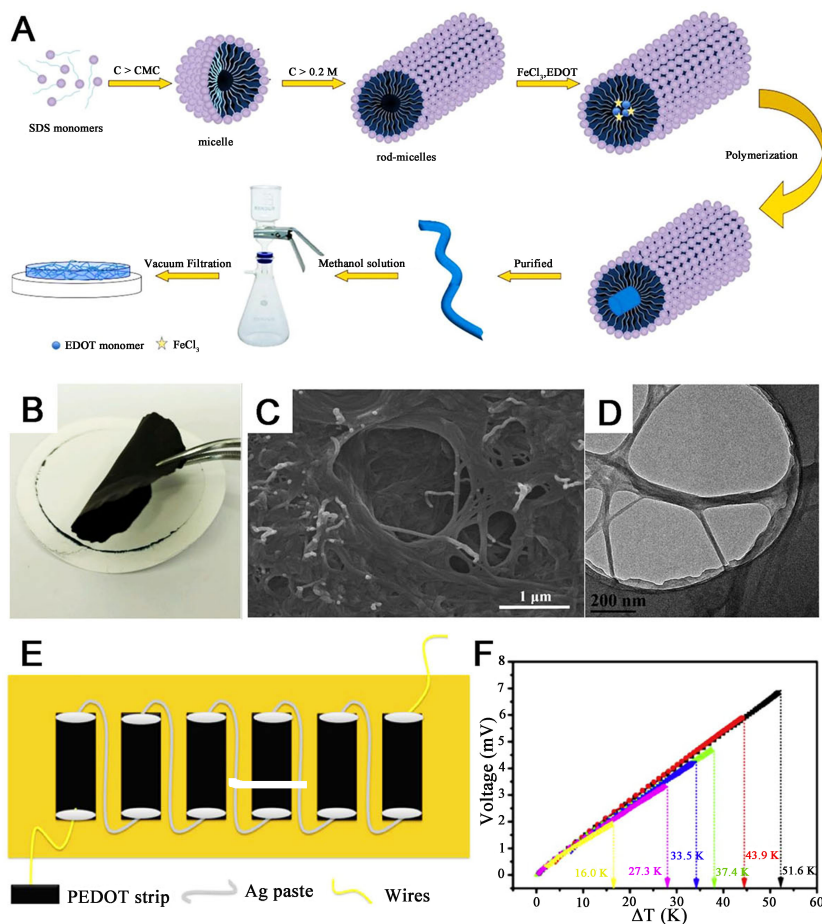


Figure 4. (A) Schematic illustration of the preparation process for synthesizing free-standing 1D PEDOT nanofiber films by a simple self-assembled micellar soft-template approach combined with a vacuum-assisted filtration method; (B) Photographs of free-standing and flexible PEDOT nanofiber films; (C) SEM and (D) TEM images of PEDOT nanofibers. Reproduced with permission from Ref^[37]. Copyright © 2021. Elsevier; (E) A schematic plot of the prototype power generator; (F) TE voltage generated by the prepared generator versus ΔT . Reproduced with permission from Ref^[38]. Copyright © 2019. Elsevier. PEDOT: Poly(3,4-ethylenedioxythiophene); SEM: scanning electron microscope; TEM: transmission electron microscopes.

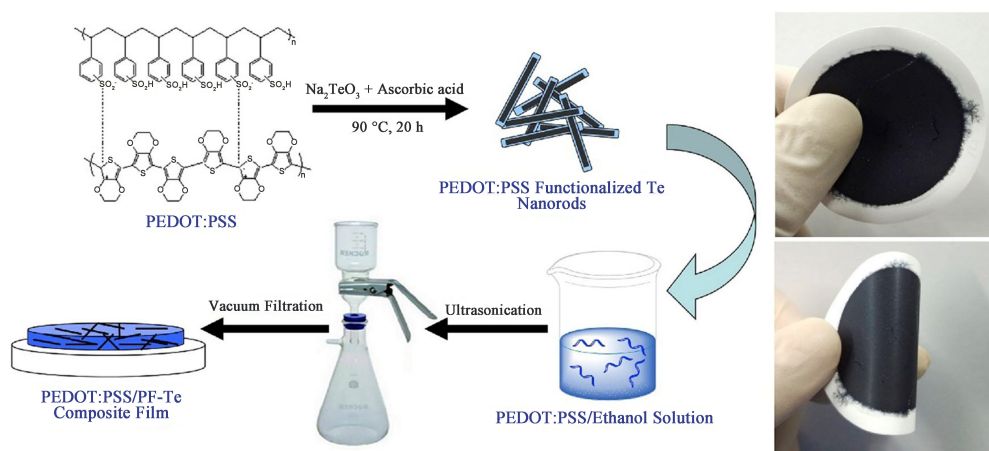


Figure 5. Schematic illustration of the flexible PEDOT:PSS/PF-Te composite film fabrication on PVDF via a filtration process. Reproduced with permission from Ref^[41]. Copyright © 2017. Elsevier. PEDOT:PSS: Poly(3,4-ethylenedioxythiophene):poly(4-styrenesulfonic acid); PF-Te: PEDOT:PSS-functionalized Te; PVDF: polyvinylidene fluoride.

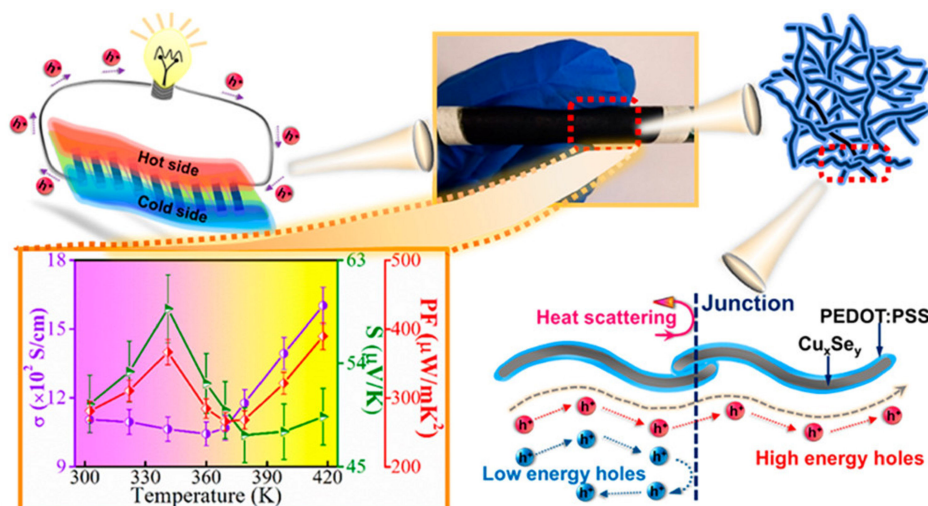


Figure 6. The flexibility of a PEDOT:PSS/Cu_xSe_y nanocomposite film and its TE properties. Reproduced with permission from Ref.^[43] Copyright © 2021. American Chemical Society. PEDOT:PSS: Poly(3,4-ethylenedioxythiophene):poly(4-styrenesulfonic acid); TE: thermoelectric.

further optimize the TE performance and flexibility of the composite films^[44]. Moreover, the highest power factor was 820 μW/mK² at 400 K, which is three times higher than that of the non-hotpressed sample. TE properties of PEDOT:PSS/Bi-Te-based alloy nanosheets^[45], PEDOT:PSS/Cu₂S^[46], PEDOT:PSS/SnSe^[47], PEDOT:PSS/MoS₂^[48], PEDOT:PSS/SiC NWs^[49], and PEDOT:PSS/silicon dioxide nanoparticles^[50] composite films prepared using similar vacuum filtration method are also reported.

Except for the PEDOT:PSS solution, PEDOT NWs synthesized by a self-assembled micellar soft-template method also show good film-forming properties due to their 1D nanostructures. For example, Tian *et al.* used Bi₂Te₃ powders and Bi₂Te₃ NWs as inorganic fillers to prepare PEDOT NW/Bi₂Te₃ nanocomposite films by a vacuum filtration method^[51]. The PEDOT NW/Bi₂Te₃ NW nanocomposite showed a higher power factor of 9.06 μW/mK² when compared to PEDOT NW/Bi₂Te₃ powders, indicating that incorporating one-dimensional NWs into the polymer matrix is more effective in improving the TE properties of conducting polymers. Liu *et al.* prepared PEDOT NW/Te NW nanocomposite films through a similar method, and the Seebeck coefficient of the composite increased from 10.08 μV/K to 89.52 μV/K with 90 wt% Te content^[52].

Table 1 summarizes the room-temperature TE properties of PEDOT/inorganic composite films. Overall, the PEDOT-based composites prepared through the vacuum filtration method mentioned above help to improve the TE properties of PEDOT. The obtained TE performances are comparable to those of PEDOT/inorganic composite films prepared from other methods, such as PEDOT:PSS/Bi₂Te₃ NW composite films obtained from a drop-casting method of a mixed solution with a power factor of 10.6 μW/mK²^[53], and PEDOT:PSS/SnS prepared by drop coating with a power factor of 43.11 μW/mK²^[54]. However, the general problem is that most of the Seebeck coefficients of composites are in the range of 10-25 μV/K, which is much lower than that of the original intention of designing (the Seebeck coefficient of pure PEDOT is about 15 μV/K). The main reason is the big difference in structure and properties between polymer and inorganic materials. Composites prepared by traditional physical mixing methods usually suffer from the problem of weak interaction between two phases, poor compatibility, low interface stability, mismatched electrical properties, and easy-to-appear phase separation. Therefore, optimizing the preparation method by various physical or chemical processes to improve the interaction between conducting polymers and the inorganic filling phases in the composite and improve the compatibility and interfacial stability between the two steps will be an effective way to enhance the TE properties of conducting polymer/inorganic nanocomposites.

Table 1. Room-temperature TE properties of PEDOT/inorganic composite films

Materials	Preparation method	S ($\mu\text{V/K}$)	σ (S/cm)	PF ($\mu\text{W/mK}^2$)	ZT	Ref.
PEDOT:PSS/PF-Te	Wet-chemical process	~	~	51.4	0.076	[41]
PEDOT:PSS/Ag ₂ Te	Wet-chemical process	-62.3	369.3	143.3	~	[42]
PEDOT:PSS/Cu _x Se _y	Wet-chemical process, cold pressing	50.8	1,047.1	270.3	~	[43]
PEDOT:PSS/Cu ₂ Se	Wet-chemical process, hot pressing	78.2	470	287.4	~	[44]
PEDOT:PSS/Bi-Te-based alloy	Lithium intercalation	20.7	1,223.8	52.3	~	[45]
PEDOT:PSS/Cu ₂ S	Cold pressing	~	~	111.54 (393 K)	~	[46]
PEDOT:PSS/SnSe	Vacuum filtration	~	~	24.42 (353 K)	~	[47]
PEDOT:PSS/MoS ₂	Liquid-phase exfoliate	19.5	1,250	45.6	0.04	[48]
PEDOT:PSS/SiC-NWs	Vacuum filtration	20.3	3,113	128.3	0.17	[49]
PEDOT:PSS/SiO ₂	Vacuum filtration	24.2	1,131.9	66.29	~	[50]
PEDOT NWs/ Bi ₂ Te ₃ NWs	Wet-chemical process	10.8	776.52	9.06	~	[51]
PEDOT NWs/Te NWs	Wet-chemical process	89.52	72.41	58.03	~	[52]

NW: Nanowire; PEDOT: poly(3,4-ethylenedioxythiophene); PEDOT:PSS: poly(3,4-ethylenedioxythiophene):poly(4-styrenesulfonic acid); PF: PEDOT:PSS-functionalized; TE: thermoelectric; ZT: thermoelectric figure of merit.

Conducting polymer/carbon nanoparticle composite TE materials

Carbon nanoparticles, including graphene (GN) and CNTs, have been considered as promising candidates to prepare conducting polymer-based composite materials through the vacuum filtration method owing to their high electrical conductivities and decent Seebeck coefficient, which can remarkably improve the TE performance of composite^[55-57]. On the one hand, their large active conjugated fused aromatic ring systems and the large specific surface areas can promote interfacial contacts between carbon nanoparticles and conducting polymers significantly, thus resulting in a synergistic effect of the components. On the other hand, the high thermal conductivities of the carbon nanoparticles can be mitigated by the conducting polymers (usually with thermal conductivities of $\sim < 1$ W/mK) wrapping or connection. Therefore, conducting polymer/carbon nanoparticle TE composites has received increasing attention.

Early in 2015, Xiong *et al.* fabricated highly conductive PEDOT:PSS/graphene composite films via vacuum filtration, and the sample containing 3 wt% graphene in N,N-Dimethylformamide (DMF) showed a power factor of 38.6 $\mu\text{W/mK}^2$. Subsequently, a hydrazine treatment was used to further optimize the TE performance of the composite, and finally, an estimated ZT value of 0.05 was obtained at room temperature [Figure 7]^[58]. In another work, they fabricated PEDOT:PSS/SWCNT composite films using a similar process, and the composites showed an increasing trend with the increase of SWCNT content^[59]. An optimized power factor of 105 $\mu\text{W/mK}^2$ was obtained at 60 wt% SWCNTs. And despite the high intrinsic thermal conductivity ($\sim 1,000$ W/mK^[60,61]) of SWCNTs, the composite retained a low polymer-like thermal conductivity around 0.15 to 0.36 W/mK due to less favorable paths for thermal energy transport caused by the PEDOT:PSS connection between tube-tube junctions; therefore, a maximum ZT value of 0.12 was obtained. Also, the TE properties of some other PEDOT:PSS/SWCNTs and PEDOT:PSS/GN composite films fabricated by a similar vacuum filtration process with different post-treatment techniques were reported^[62-65]. For example, Deng *et al.* prepared free-standing PEDOT:PSS/SWCNT composite films with an ionic liquid (IL) treatment using a vacuum filtration method [Figure 8]^[64]. The ion-exchange effect and promotion of SWCNT dispersion by the IL realized a synergistic boost of electrical conductivity and a Seebeck coefficient. The maximum power factor reached 182.7 ± 9.2 $\mu\text{W/mK}^2$ at room temperature. Another

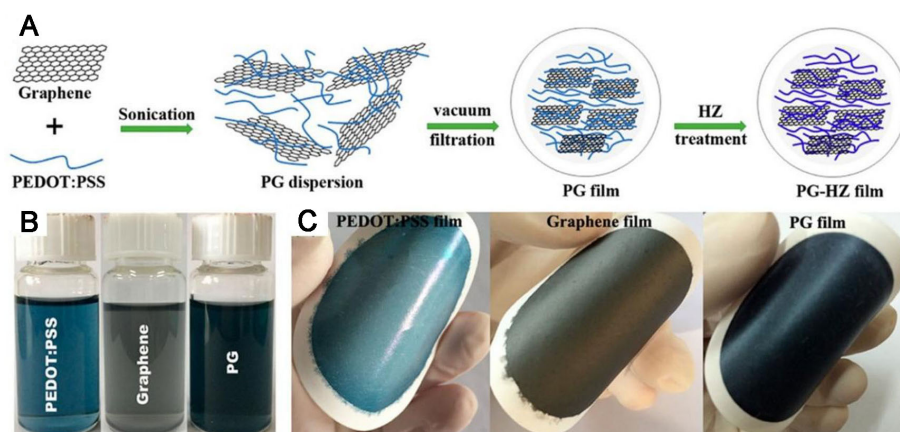


Figure 7. (A) Schematic illustration of the preparation and hydrazine-treatment process of the PEDOT:PSS/graphene composite films; (B) Photographs of dispersion of PEDOT:PSS, graphene, and PEDOT:PSS/graphene in DMF after sonication; (C) Photos of PEDOT:PSS, graphene, and PEDOT:PSS/graphene films. Reproduced with permission from Ref^[58]. Copyright © 2015. American Chemical Society. DMF: N,N-Dimethylformamide; PEDOT:PSS: poly(3,4-ethylenedioxythiophene):poly(4-styrenesulfonic acid).

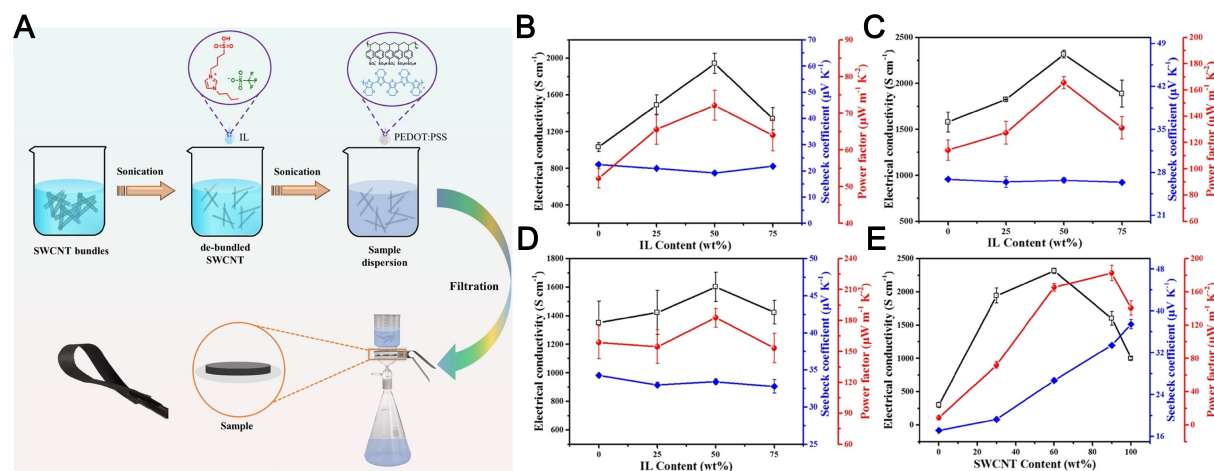


Figure 8. (A) Schematic illustration of the preparation procedures of the PEDOT:SWCNT composites with the IL; (B-E) Dependences of TE performance on IL content for PEDOT:PSS/SWCNT composites with different SWCNT contents: (B) 30 wt% SWCNT; (C) 60 wt% SWCNT; and (D) 90 wt% SWCNT; (E) dependence of TE performance on SWCNT content for the PEDOT:PSS/SWCNT-IL50 composite. Reproduced with permission from Ref^[64]. Copyright © 2021. American Chemical Society. PEDOT:PSS: Poly(3,4-ethylenedioxythiophene):poly(4-styrenesulfonic acid); SWCNT: single-walled carbon nanotube; TE: thermoelectric.

fantastic property of CNTs is that their conduction type can be easily converted from p- to n-type through the n-type doping method by different reducing agents^[66,67]. Then Song *et al.* prepared flexible and lightweight TEGs by vacuum filtrated PEDOT:PSS/SWCNTs as p-type materials and polyethyleneimine-doped SWCNTs as n-type materials, respectively^[68].

Liang *et al.* have researched the TE properties of conducting polymer/carbon nanoparticle composite prepared by combining chemical oxidative polymerization and vacuum filtration. For example, a large-area stretchable, super flexible, and mechanically stable PPy/SWCNT film with a diameter of ~18 cm was achieved by an *in situ* chemical oxidative polymerization of pyrrole monomer in the SWCNT solution, followed by vacuum filtration^[69]. Further, they designed a unique layered morphology containing nanosheets of SWCNTs sandwiched by PPy NWs via physical mixing and vacuum filtration in different

dispersion mediums^[70]. The composite films with the layered morphology revealed dramatically improved TE performances with a power factor of $21.7 \pm 0.8 \mu\text{W}/\text{mK}^2$ for the sample containing 60 wt% SWCNTs using an SDBS dispersion medium. Also, PEDOT-tosylate (PEDOT-Tos)/acidified-SWCNT composites with greatly intensified TE performance are fabricated by combining chemical oxidative polymerization, acid treatment of SWCNTs, and vacuum filtration^[71]. Due to the formation of a highly conductive network between the PEDOT-Tos polymer chains and SWCNTs, along with the acid doping process, the composites showed an electrical conductivity as high as $4,731.6 \pm 42.3 \text{ S}/\text{cm}$, which contributed to the improvement of the TE performance. Xiang *et al.* reported the TE properties of polyaniline (PANI)/GN nanocomposites prepared by *in situ* polymerization of aniline monomer in the presence of GN, following a vacuum filtration process^[24]. The addition of GN improved the electrical conductivity of the nanocomposite, and the Seebeck coefficient changed with the initial concentration of aniline in the solution and the protonation of PANi. Therefore, the *ZT* value of the nanocomposite was two orders of magnitude higher than either of the constituents.

To sum up, the conducting polymer/carbon nanoparticle composite films usually show significantly enhanced TE properties, and the enhancement is mainly ascribed to the strong π - π interaction between conducting polymers and carbon nanoparticles. Other methods also show similar results; for example, Zhang *et al.* prepared PEDOT:PSS/SWCNTs composite films by a doctor-blade process, followed by a DMSO doping treatment, and the composite film with 74 wt% SWCNT showed a power factor of $300 \mu\text{W}/\text{mK}^2$ ^[72]; Wang *et al.* prepared PANI/GN composite films by a combination of *in situ* polymerization and drop-casting processes, and more ordered regions were formed in the PANI/ GN composite due to the strengthened π - π conjugation interactions, leading to a maximum power factor of $55 \mu\text{W}/\text{mK}^2$ ^[56]. However, the preparation process of these methods usually includes a wet-chemical or post-treatment process and is not convenient compared with the vacuum filtration methods.

CARBON NANOPARTICLE-BASED TE MATERIALS

Pure carbon nanoparticle TE materials

Carbon nanoparticles, especially GN and CNTs, show good film-forming properties because of their 2D and 1D nanostructures. Besides, carbon nanoparticles usually present good electrical conductivities. Therefore, GN and CNTs fabricate free-standing TE films by a vacuum filtration method. For example, p-type and n-type CNT bucky papers were prepared by the acid treatment or reduction through PEI of vacuum-filtrated CNT films^[73]. The acid-treated SWCNTs generated a positive thermopower of $60 \mu\text{V}/\text{K}$ at 380 K. The PEI-SWCNT caused a negative thermopower of $-60 \mu\text{V}/\text{K}$ at 380 K. Then, a TE module composed of four p-n layers was fabricated. It showed a voltage of 7 mV under a temperature gradient of 50 K. Kim *et al.* used a hybrid filler of GN SWCNTs to prepare a TE device with p-type TE film and n-type bucky paper^[74]. The p-type TE film had a composition ratio of carbon filler (GN:SWCNT, 8:2), PVDF, and IL of 1:1:1. And n-type TE bucky paper was made with a filtration method with GN and SWCNTs followed by a PEI solution treatment. The thermocouple composed of 22 p-n legs showed an output power value of 14.9 nW with a temperature difference of 10 K.

Usually, the as-grown SWCNTs possess different chirality, and the unseparated SWCNTs contained $\sim 2/3$ of semiconducting and $\sim 1/3$ of metallic nanotubes^[75]. The electronic and bandgap structures of metallic SWCNTs and semiconducting SWCNTs are very different^[76-78], leading to various electronic transport properties and TE performance for SWCNT- and CNT-based composites. Thus, it is vital to investigate the electronic and TE properties of separated CNTs. Using an aqueous two-phase extraction method, Tambasov *et al.* prepared semiconducting and metallic SWCNT dispersions from commercialized SWCNTs^[79] [Figure 9]. Then, using vacuum filtration, thin films based on unseparated, semiconducting,

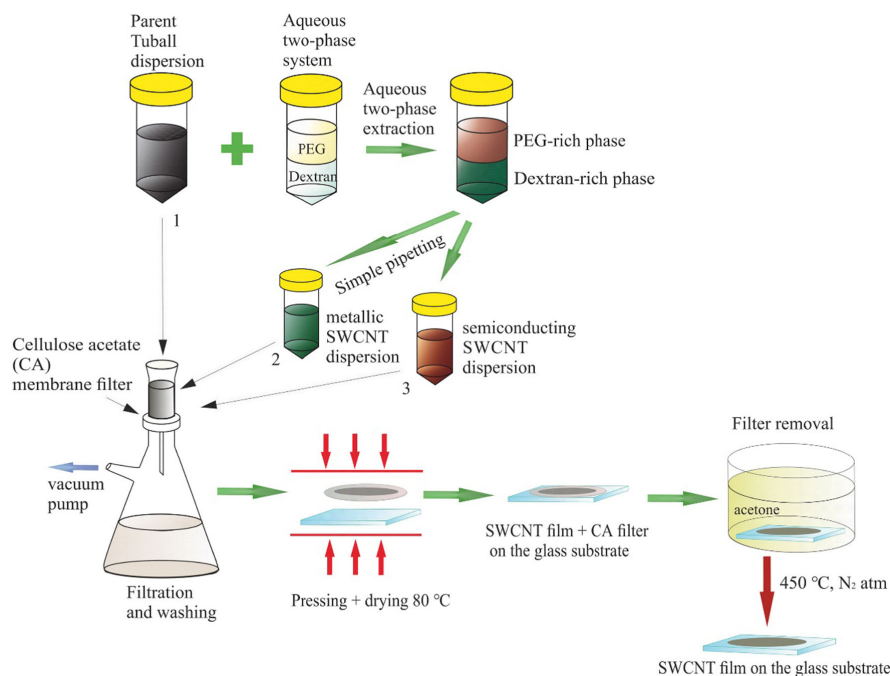


Figure 9. Schematic diagram of the formation process of thin SWCNT films on glass substrates. Reproduced with permission from Ref^[79]. Copyright © 2019. Elsevier. PEG: Polyethylene glycol; SWCNT: single-walled carbon nanotube.

and metallic SWCNTs were formed from the appropriate distributions. The unseparated SWCNTs showed the highest electrical conductivity, and the semiconducting SWCNTs showed the highest Seebeck coefficient of $\sim 80 \mu\text{V/K}$ with a low electrical conductivity at room temperature. Finally, the power factors for metallic SWCNTs and unseparated SWCNT films were correspondingly 47 and $213 \mu\text{W/mK}^2$.

Wu *et al.* used multi-walled CNTs (MWCNTs) to prepare the CNT films by the CVD method and vacuum filtration, and then the films were piled up to fabricate anisotropic 3D CNT sponges with different CNT film layers^[80]. The anisotropic TE properties were studied, and due to the small size of pores and the low thermal conductivity of CNTs along the radial direction, the cross-plane value of ZT (ZT_{\perp}) is much larger than that along the in-plane direction (ZT_{\parallel}). This significant anisotropic thermal conduction of CNT films is a primary factor that restrains the TE conversion using the Seebeck effect since the temperature gradient is challenging to maintain in the current flow direction^[81,82]. So, Matsumoto *et al.* introduced polystyrene particles as orientation aligners during the film formation process by vacuum filtration to control the orientation of the CNTs^[82]. Through anisotropy control, the through-plane thermal and electrical conductivity of SWCNT films increased due to the increased SWCNTs oriented in the through-plane direction. Consequently, the sizeable in-plane anisotropy was decreased for thermal and electrical conductivity. The GN paper, composed of a bilayer and a few layers of GN, was fabricated through an electrochemical exfoliation and vacuum filtration process by Gee *et al.*^[83]. Then, the anisotropic thermal conductivity of the GN paper was investigated. Due to the highly oriented order of the basal plane rather than the horizontal direction, the in-plane thermal conductivity measured by the TE method was $3,390 \text{ W/mK}$, which is several orders of magnitude higher than that of the cross-plane.

Carbon nanomaterials/inorganic composite TE materials

Although inorganic TE materials usually show a high power factor, their flexibility could be better. Even by reducing dimensionality and size, it is hard for inorganic TE materials to fabricate flexible films by

themselves^[84]. Because of the unique structural characteristics and extraordinary mechanical, electrical, and thermal properties, carbon nanomaterials are used to prepare carbon nanomaterials/inorganic composite TE materials, aiming to combine the excellent electrical properties and flexibility of carbon nanomaterials with the high power factor (especially for the Seebeck coefficient) of inorganic TE materials to achieve ideal TE performances.

In 2013, Bark *et al.* prepared CNT/Bi₂Te₃ composites by dispersing Bi₂Te₃ particles and CNTs in a solvent, followed by vacuum filtration^[85]. Then, the influence of CNTs on the electrical conductivity and Seebeck coefficient of composites were studied. With low CNT contents, the electrical conductivity and Seebeck coefficient were slightly increased by the p-doping effect of CNTs on Bi₂Te₃ particles. Moreover, with the increased amount of CNTs, the electrical conductivity and Seebeck coefficient of composites were decreased due to the enhanced development of hindered carrier mobility. The highest power factor for the composite was about 140 $\mu\text{W}/\text{mK}^2$, which contained 20 V% CNTs. Similarly, Chen *et al.* prepared a series of n-type flexible SWCNT/Bi₂Te₃ composite films on PVDF membranes by *in situ* growth of Bi₂Te₃ nanosheets on SWCNTs assisted by poly(vinylpyrrolidone) (PVP) through a solvothermal method and subsequent vacuum filtration^[86]. The morphology and structure of the SWCNT/Bi₂Te₃ composite films indicated that Bi₂Te₃ was successfully grown on the SWCNT network [Figure 10]. When the mass ratio of SWCNTs to Bi₂Te₃ was 1:0.8, the composite film showed a high electrical conductivity of 244.6 S/cm at room temperature, and a power factor of 57.8 $\mu\text{W}/\text{mK}^2$ was obtained at 386 K. This work provides a convenient way to prepare flexible and n-type TE composite films. Fan *et al.* first prepared 2D SnSe nanobelts by a chemical exfoliation process. Then, free-standing SWCNT/SnSe nanobelt composite films were obtained *via* a facile solution mixing and subsequent vacuum filtration process^[87]. A post-treatment of thermal annealing was used to further improve the TE performance of the composite. Finally, a maximum power factor reached $145 \pm 28 \mu\text{W}/\text{mK}^2$ at room temperature when the sample contained 80 wt% SWCNTs, which is much higher than the power factors observed in either individual component. Gao *et al.* fabricated highly flexible composite films based on reduced graphene oxide (rGO) and Te NWs by vacuum filtration^[88]. Due to the combination of the high carrier mobility of Te NWs and the high carrier concentration of rGO, the electrical conductivity and Seebeck coefficient of the optimized composite film could reach 978 S/m and 286 $\mu\text{V}/\text{K}$, respectively, resulting in a power factor of 80 $\mu\text{W}/\text{mK}^2$ at 40 °C. Xiao *et al.* prepared flexible n-type rGO/Ag₂Se NW composite films by vacuum filtration and cold-pressing treatment^[89]. The composite film showed the highest power factor of 228.88 $\mu\text{W}/\text{mK}^2$ at 331 K for the sample with 0.01 wt% rGO. Besides, the low electrical conductivity of conducting metal-organic frameworks (MOF) has limited their application in TE devices. Then, free-standing SWCNT/MOF [Ni-1,2,5,6,9,10-triphenylenehexathiol (THT)] composite films were fabricated by the vacuum filtration method^[90]. Because of the covalent bond between SWCNTs and MOFs, the conductive MOFs were successfully grafted onto the surface of SWCNTs. The composite film showed a maximum PF of $\sim 98.1 \mu\text{W}/\text{mK}^2$ at 4 wt% SWCNT loading, which was considerably higher than that of the pristine Ni-THT. The room-temperature TE properties of carbon nanomaterials/inorganic composite films are listed in Table 2.

FLEXIBLE INORGANIC TE MATERIALS

Ag₂Se-based TE materials

Although conducting polymer-based and carbon nanomaterial-based composites show good flexibility, obtaining TE performances comparable to inorganic counterparts is still a significant challenge. Inorganic semiconductors, such as Bi₂Te₃, SnSe, and Ag₂Se, usually show high TE performance, while the inherent rigidity and brittleness have limited their application as flexible TE devices^[91]. Ding *et al.* have developed a simple, low-cost process to prepare inorganic semiconductors with high TE properties and excellent flexibility^[92].

Table 2. Room-temperature TE properties of carbon nanomaterials/inorganic composite films

Materials	Preparation method	S ($\mu\text{V}/\text{K}$)	σ (S/cm)	PF ($\mu\text{W}/\text{mK}^2$)	ZT	Ref.
$\text{Bi}_2\text{Te}_3/\text{MWCNTs}$	Ball-milling	-128	-80	140	-	[85]
$\text{Bi}_2\text{Te}_3/\text{SWCNTs}$	Solvothermal method	-36.3	244.6	32.3	-	[86]
$\text{SnSe}/\text{SWCNTs}$	Lithium intercalation, thermal annealing	49	588 ± 12	145 ± 28	0.003	[87]
rGO/Te NWs	Solvothermal method	9.78	286	80 (313 K)	-	[88]
rGO/Ag ₂ Se NWs	Wet-chemical approach, cold pressing	-111.72	183.37	228.88 (331 K)	-	[89]
MOFs/SWCNTs	Vacuum filtration	-	-	98.1	0.037	[90]

NWs: Nanowires; MOFs: metal-organic frameworks; TE: thermoelectric; ZT: thermoelectric figure of merit; MWCNTs: multi-walled carbon nanotubes; rGO: reduced graphene oxide; SWCNTs: single-walled carbon nanotubes.

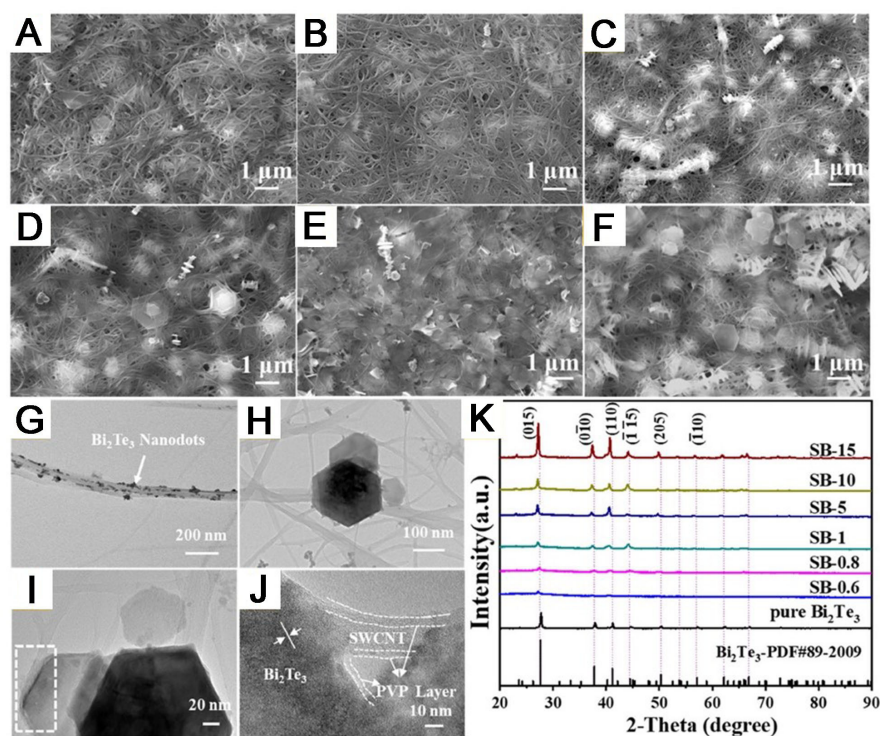


Figure 10. (A-F) SEM images of SWCNT/ Bi_2Te_3 composite films, corresponding to mass ratios of the SWCNTs to Bi_2Te_3 -0.6/0.8/1/5/10/15; (G-J) HRTEM of SWCNTs@ Bi_2Te_3 -5; (K) XRD patterns of a series of SWCNT@ Bi_2Te_3 films, pristine Bi_2Te_3 power, and pristine SWCNT film. Reproduced with permission from Ref^[86]. Copyright © 2021. American Chemical Society. HRTEM: High-resolution transmission electron microscopy; SEM: scanning electron microscope; SWCNT: single-walled carbon nanotube; XRD: X-ray diffraction analysis.

A series of pioneering works were reported on the optimization of the process, analysis of microstructures, and transmission mechanisms on TE properties of Ag_2Se -based materials. In 2019, researchers first synthesized Ag_2Se NWs, then the NWs were vacuum-filtrated onto a nylon membrane and finally hot pressed at 200 °C and 24 MPa^[92]. The Ag_2Se film displayed a power factor of $987.4 \pm 104.1 \mu\text{W}/\text{mK}^2$ at 300 K with an estimated ZT value of 0.6 [Figure 11]. The high TE performance was mainly attributed to the particular Ag_2Se film. The Ag_2Se film showed excellent flexibility, and 93% of the original electrical

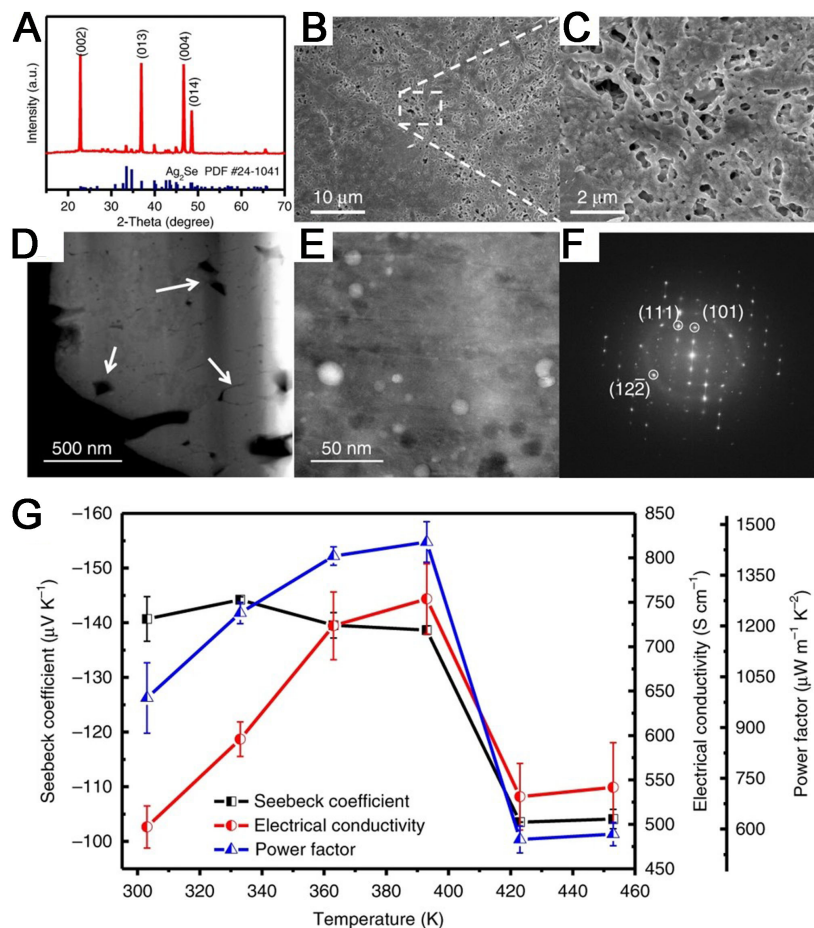


Figure 11. (A) XRD pattern of the Ag_2Se film; (B) Low magnification FESEM image of Ag_2Se film; (C) High magnification FESEM image of Ag_2Se film; (D) Overview high-angle annular dark field-STEM image; (E) Typical STEM image; (F) FFT image corresponding to (E); (G) Temperature dependence of Seebeck coefficient, electrical conductivity, and power factor for the Ag_2Se film. Reproduced with permission from Ref.^[92]. Copyright © 2019. Springer Nature. FESEM: Field emission scanning electron microscopy; FFT: fast Fourier transform; STEM: scanning transmission electron microscopy; XRD: X-ray diffraction analysis.

conductivity was retained after 1,000 bending cycles around an 8-mm diameter rod. This excellent flexibility came from the synergetic effect of the nylon membrane and the Ag_2Se film intertwined with numerous high aspect-ratio Ag_2Se grains. Suitable element doping treatment improves the TE performance of Ag_2Se ^[93]. Therefore, they studied the influence of different elements (including Ga, S) doping on the TE properties of flexible Ag_2Se films^[94,95].

To solve the high porosity and control the growth direction of the as-prepared Ag_2Se film, they optimized the synthesis temperature of Ag_2Se NWs from room temperature to 40 °C. They kept the other process conditions the same as Refs.^[92,96]. The morphology synthesized Ag_2Se changed from uniform NWs to multisized nanostructures, leading to a more compact film (~90% relative density) after hot pressing with a suppressed growth direction along the (00l). Finally, the power factor of the optimized Ag_2Se film increased to 1,882 $\mu\text{W}/\text{mK}^2$ at 300 K, which is nearly twice as large as the previous report. However, the high density limited the flexibility of the film, and the power factor decreased by 16.1% after bending 1,500 times due to the break of some weak-bonded Ag_2Se grain boundaries. To solve the problem, they introduced PVP as a binder to hinge rigid Ag_2Se micro grains to improve the flexibility and take full advantage of the intrinsic low thermal conductivity of PVP to increase the ZT value of the Ag_2Se film^[97]. The microstructure

characterizations indicated that the PVP was mainly located at the wall of micropores, and most Ag_2Se grains have coherent interfaces [Figure 12]. Then, an optimal film exhibited a power factor as high as $\sim 1,910 \mu\text{W}/\text{mK}^2$ (corresponding $ZT \sim 1.1$) at 300 K and excellent flexibility (only a 5.5% decline in power factor after 1,000 times bending around a 4 mm radius rod). They also developed a one-pot method to synthesize Ag_2Se powder instead of the Se NW template method. Then, the Ag_2Se film was prepared by vacuum filtration, followed by hot pressing^[98]. Compared to the template method, the new approach is much simpler, requires a significantly shorter time, has a higher yield, and is more environmentally friendly. By adjusting the synthesis process of Ag_2Se powder, an optimal power factor could reach $\sim 2,043 \mu\text{W}/\text{mK}^2$. Besides, TE properties of flexible $\text{Ag}/\text{Ag}_2\text{Se}$ composite films with different $\text{Ag}:\text{Se}$ ratios prepared by other methods were also reported^[99,100], and the TE performances were listed in Table 3. Wu *et al.* fabricated n-type $\text{Ag}_2\text{Se}/\text{Ag}$ composite films using a similar method. They investigated the influence of Ag particle size on the TE properties of the composite film through the adjustment of the sequence and reaction time of the reducing agent L-ascorbic acid^[101]. After optimization, the flexible composite film showed a power factor as high as $2,277.3 \mu\text{W}/\text{mK}^2$. Palaporn *et al.* fabricated bacterial cellulose (BC)/ Ag_2Se nanocomposite films by blending BC with Ag_2Se powders, followed by vacuum filtration and hot pressing^[102]. The electrical conductivity and Seebeck coefficient of the nanocomposites varied with the Ag/Se proportion due to the changes in the carrier concentration and mobility. The highest power factor was $291 \mu\text{W}/\text{mK}^2$ at room temperature.

Other inorganic TE materials

Besides Ag_2Se -based materials, researchers fully utilize the convenience and film-forming aiding properties of the vacuum filtration method. Inorganic TE materials, such as Cu-Te, Cu-Se, Ag_2Te , Bi_2Te_3 , and other inorganic semiconductors, are used to prepare flexible TE films using vacuum filtration. For example, Zhou *et al.* prepared a free-standing flexible copper telluride NW/PVDF ($\text{Cu}_{1.75}\text{Te}$ NWs/PVDF = 2:1) thin film using a five-step vacuum filtration process [Figure 13]^[105]. By burying the $\text{Cu}_{1.75}\text{Te}$ NWs into the PVDF matrix, the flexible fabric exhibits a Seebeck coefficient and electric conductivity of $9.6 \mu\text{V}/\text{K}$ and $2,490 \text{ S}/\text{cm}$ at room temperature, respectively, resulting in a power factor of $23 \mu\text{W}/\text{mK}^2$. Pammi *et al.* reported Cu_{2-x}Se NW/PVDF composite flexible thin films, which achieved a power factor of $105.32 \mu\text{W}/\text{mK}^2$ ^[106]. Notably, the mechanical hot-pressing transfer process followed by vacuum filtration was found to have increased conductance due to a reduction in the junction resistance and to an interconnection density between NWs and densification compared to various fabrication methods. CuI/nylon composite films with a Seebeck coefficient as high as $600 \mu\text{V}/\text{K}$ were also prepared^[107]. Although the low electrical conductivity limited its TE performance, the quick voltage response under temperature gradient showed the potential application in wearable thermal sensors.

To improve the electrical conductivity of and maintain the initial morphology of the Ag_2Te NWs, Zeng *et al.* reported an approach to welding Ag_2Te NWs at room temperature to enhance their contacts by the combination of vacuum filtration and drop-coating methods^[108]. Under compressive stress and atomic diffusion, a diffusion weld is generated at the intersection of the NWs to form a room-temperature welded Ag_2Te NW film. The welded Ag_2Te NW film showed a carrier concentration of about one-half that of the typical Ag_2Te NW film and a carrier mobility of four times larger than that of vacuum filtration-assisted Ag_2Te NW film (with a loose connection). Finally, the welded Ag_2Te NW film showed a power factor of $359.76 \mu\text{W}/\text{mK}^2$ at 420 K, about three times larger than the vacuum-filtrated Ag_2Te NW film. Yu *et al.* fabricated a robust, flexible Ag_xTe NW film by *in situ* chemical transformation and vacuum-assisted filtration^[109]. Then, its TE performance was further optimized by adjusting the Ag/Te ratio and post-treatment pressures/pressing temperature. And the Ag_xTe NW film displayed a tensile strength of $\sim 78.4 \text{ MPa}$ with a power factor of $48.9 \mu\text{W}/\text{mK}^2$ at room temperature. Besides, the TE properties of cellulose nanofiber (CNF)/ Bi_2Te_3 composite films^[110], paper matrix-based Bi_2Te_3 and Sb_2Te_3 composite films^[111], Se

Table 3. Room-temperature TE properties of the Ag₂Se-based flexible film

Materials	Preparation method	S (μV/K)	σ (S/cm)	PF (μW/mK ²)	ZT	Ref.
Ag ₂ Se	Wet-chemical process, hot pressing	-140	497	987	0.6	[92]
Ag _{1.98} Ga _{0.02} Se	Wet-chemical process, hot pressing	-115	-880	1,162	-	[94]
Ag ₂ S _{1-y} Se _y	Wet-chemical process, hot pressing	-106	849	954.7	-	[95]
Ag ₂ Se	Optimized wet chemical method, hot pressing	-143	919	1,880	0.8	[96]
PVP coated Ag ₂ Se	In-situ synthesis, hot pressing	-143	929	1,910	1.1	[97]
Ag ₂ Se	A one-pot synthesis method, hot pressing	-150	908	2,043	-	[98]
Ag/Ag ₂ Se	Wet-chemical process, hot pressing	-68.5	3,958	1,860.6	-	[99]
Ag/Ag ₂ Se	Microwave-assisted synthesis method	-89.6	3,030	2,431	> 0.55	[100]
Ag/Ag ₂ Se	Wet-chemical process, hot pressing	-91.5	2,720.1	2,277.3	0.71	[101]
BC/Ag ₂ Se	Wet-chemical process, blending + hot pressing	-60	810	291	-	[102]
PVDF/Ag ₂ Se	Wet-chemical process, blending	-95.9	205.52	189.02	-	[103]
Ag ₂ Se	Chemical template method	-82.33	385.42	261.26	-	[104]

BC: Bacterial cellulose; TE: thermoelectric; ZT: thermoelectric figure of merit; PF: PEDOT:PSS-functionalized; PVP: poly(vinylpyrrolidone); PVDF: polyvinylidene fluoride.

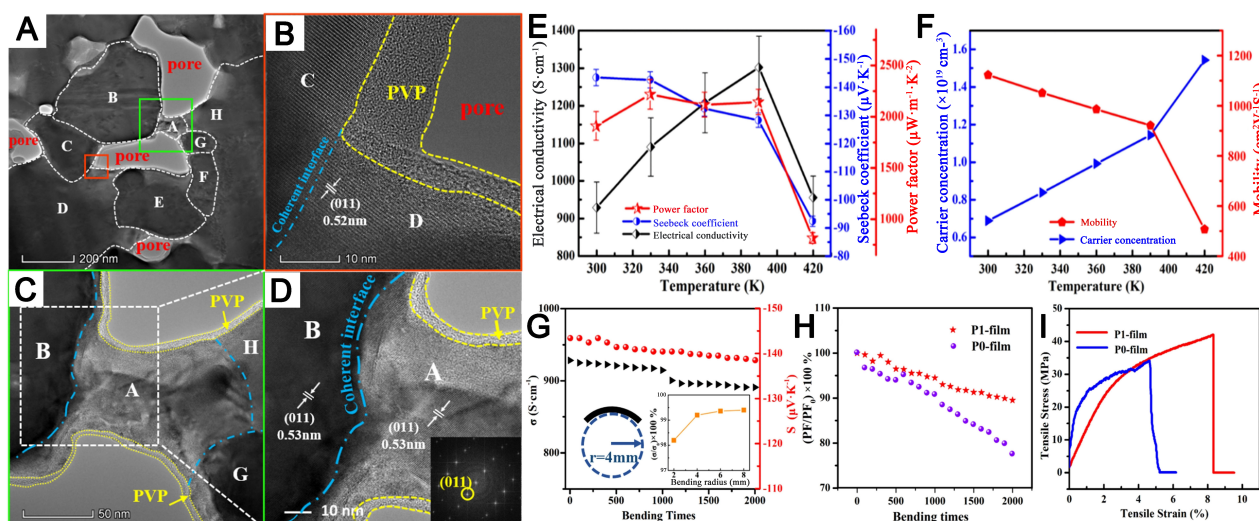


Figure 12. (A-D) Cross-sectional microstructure characterization of the PVP/Ag₂Se composite films: (A) a typical cross-sectional TEM image indicating the existence of pores surrounded by several grains (grains A-G); (B) the enlarged image of the red square marked in (A) showing a coherent interface and a PVP layer; (C) the enlarged image of the green square marked in (A) containing four Ag₂Se grains coated with PVP; (D) an HRTEM image of the white square marked in (C) containing a coherent interface, with a corresponding FFT image given in the inset; Temperature dependent (E) Seebeck coefficient, electrical conductivity and power factor; and (F) carrier mobility and concentration of the composite film; (G-I) Flexibility test of the composite film: (G) The electrical conductivity and Seebeck coefficient of the composite film as a function of bending times with a bending radius of 4 mm; (H) the degradation of power factor of the composite films as a function of bending times with a bending radius of 4 mm; (I) the stress-strain curve of the composite films (P0: hot-pressed Ag₂Se films; P1: hot-pressed PVP/Ag₂Se films). Reproduced with permission from Ref^[97]. Copyright © 2021. Elsevier. FFT: Fast Fourier transform; HRTEM: high-resolution transmission electron microscopy; PVP: poly(vinylpyrrolidone); TEM: transmission electron microscopes.

solid solution-substituted Ag₂S films^[112] prepared by vacuum filtration method are also reported, and the TE properties are listed in Table 4. All the films show good flexibility, enabling the fabrication of flexible TEGs and paving the way for the commercial application of self-powered wearable electronics.

Table 4. Room-temperature TE properties of other inorganic TE materials

Materials	Preparation method	S ($\mu\text{V/K}$)	σ (S/cm)	PF ($\mu\text{W/mK}^2$)	ZT	Ref.
Cu _{1.75} Te NWs/PVDF	Mechanical Press, drop-coating	9.6	2,490	23	~	[105]
Cu _{2-x} Se NW/PVDF	Drop casting, cold pressing	14.16	5,578.2	111.84	-0.04	[106]
CuI/Nylon	Wet-chemical process, hot pressing	600	0.09	3.03	~	[107]
Ag ₂ Te NWs	Hydrothermal	-99.48	153.35	151.76	~	[108]
Ag _x Te NWs	Room-temperature welding	-154.96	149.82	359.76	~	
Ag _x Te NWs	Hydrothermal, <i>in situ</i> chemical transformation,	-50.4	192.5	48.9	~	[109]
CNF/Bi _{0.5} Sb _{1.5} Te ₃	Vacuum filtration	154	493	1,169.2	~	[110]
CNF/Bi ₂ Se _{0.3} Te _{2.7}		-130	532	899.08	~	
Bi ₂ Te ₃ and Sb ₂ Te ₃ modified paper	Vacuum filtration	142	~	~	~	[111]
Se/Ag ₂ S	Wet-chemical process, hot pressing	-81.4	743	492.6	> 0.26	[112]

CNF: Cellulose nanofiber; NWs: nanowires; TE: thermoelectric; ZT: thermoelectric figure of merit; PF: PEDOT:PSS-functionalized; PVP: poly(vinylpyrrolidone); PVDF: polyvinylidene fluoride.

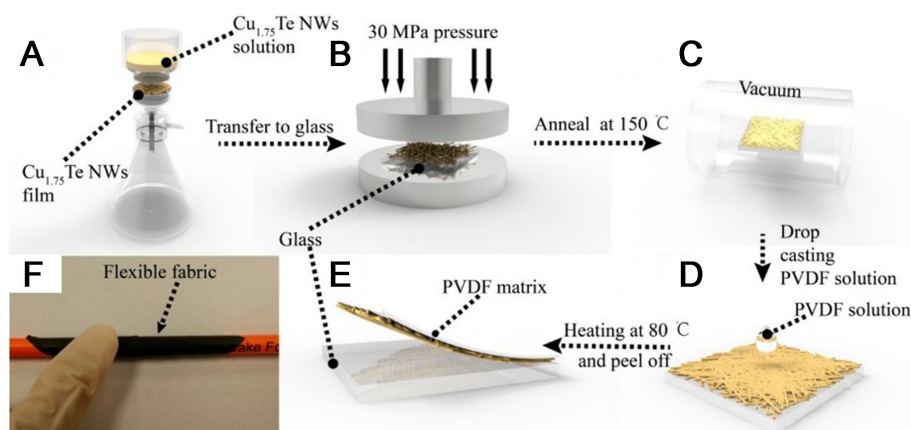


Figure 13. Schematic diagram of the preparation process for the flexible Cu_{1.75}Te NW/PVDF TE fabric, including (A) vacuum filtration; (B) mechanical pressing; (C) annealing; (D) drop-coating PVDF solution upon the film; and (E) peeling off the NW/PVDF film; (F) The roll-up photograph of the fabricated Cu_{1.75}Te NW/PVDF film. Reproduced with permission from Ref^[105]. Copyright © 2015. American Chemical Society. NW: Nanowire; PVDF: polyvinylidene fluoride; TE: thermoelectric.

TWO-DIMENSIONAL TE MATERIALS

Two-dimensional materials have unique state densities with confined electrons and holes, making them promising TE materials. Due to its high in-plane carrier mobility (200-500 cm²/Vs) and low thermal conductivity (0.1-1 W/mK), MoS₂ has attracted wide attention. In 2016, Wang *et al.* prepared exfoliated bulk MoS₂ by lithium intercalation and obtained the restacked MoS₂ thin film using a filtration technique^[113]. The maximum Seebeck coefficient reached 93.5 $\mu\text{V/K}$; the highest $ZT = 0.01$ was calculated. Also, this method could be imitated on other transitional metal dichalcogenides. Piao *et al.* synthesized 1T phase WS₂ nanosheets through hydrothermal methods and fabricated flexible WS₂ thin films by vacuum filtration with an electrical conductivity of 45 S/cm and a Seebeck coefficient of 30 $\mu\text{V/K}$ ^[114]. After thermal annealing, the electrical conductivity was enhanced to 120 S/cm while not lowering the Seebeck coefficient, resulting in an optimized power factor of 9.40 $\mu\text{W/mK}^2$. Then, they reported a bottom-up hydrothermal route to prepare 1T-WS₂/SWCNT hybrid composites with 3D architecture in which 1D SWCNT nanotubes and 2D WS₂ nanosheets interweaving^[115]. Enhanced electrical conductivity and Seebeck coefficients were obtained by introducing SWCNTs into 1T-WS₂. Flexible thin films with an impressive power factor of

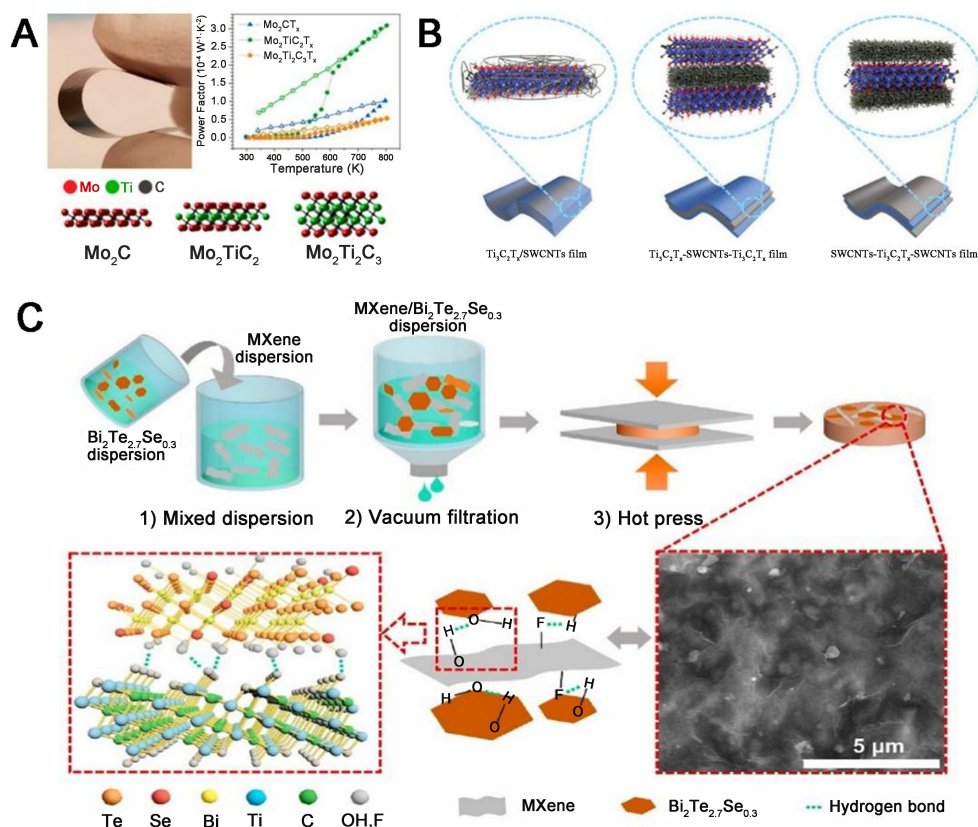


Figure 14. (A) TE properties of two-dimensional molybdenum-based MXenes. Reproduced with permission from Ref^[22]. Copyright © 2017. American Chemical Society; (B) The schematic structure diagrams of $\text{Ti}_3\text{C}_2\text{T}_x/\text{SWCNT}$, $\text{Ti}_3\text{C}_2\text{T}_x\text{-SWCNT-Ti}_3\text{C}_2\text{T}_x$ and $\text{SWCNT-Ti}_3\text{C}_2\text{T}_x\text{-SWCNT}$ films. Reproduced with permission from Ref^[116]. Copyright © 2020. John Wiley and Sons; (C) Schematic demonstration of the preparation process of $\text{Bi}_2\text{Te}_{2.7}\text{Se}_{0.3}/\text{Ti}_3\text{C}_2\text{T}_x$ composites. Reproduced with permission from Ref^[117]. Copyright © 2022. Elsevier. TE: Thermoelectric; SWCNT: single-walled carbon nanotube.

$61.70 \mu\text{W}/\text{mK}^2$ were fabricated using a facile vacuum filtration technique.

MXenes have attracted widespread attention as two-dimensional materials containing transition metal carbides and nitrides. In 2017, Kim *et al.* employed vacuum-assisted filtration to prepare three free-standing MXenes (Mo_2CT_x , $\text{Mo}_2\text{TiC}_2\text{T}_x$, and $\text{Mo}_2\text{Ti}_2\text{C}_3\text{T}_x$) films [Figure 14A]^[22], which exhibit n-type Seebeck coefficients and high electrical conductivity upon heating to 800 K. For the $\text{Mo}_2\text{TiC}_2\text{T}_x$ MXene, the power factor reached $3.09 \times 10^{-4} \text{ W}/\text{mK}^2$ at 803 K. Then, Ding *et al.* reported that a practical heterostructure design could effectively improve the TE performance of MXenes [Figure 14B]^[116]. Layered composite films with 2D-3D sandwich structures consisting of 2D MXenes and 1D SWCNTs were prepared by vacuum-assisted filtration. The $\text{Ti}_3\text{C}_2\text{T}_x\text{-SWCNTs-Ti}_3\text{C}_2\text{T}_x$ film displayed considerable electrical conductivity of 750.9 S/cm and an enhanced Seebeck coefficient of $-32.2 \mu\text{V}/\text{K}$. Compared to $\text{Ti}_3\text{C}_2\text{T}_x/\text{SWCNT}$ films with interlaced structures, the $\text{Ti}_3\text{C}_2\text{T}_x\text{-SWCNTs-Ti}_3\text{C}_2\text{T}_x$ film shows a higher power factor, 25 times higher than that of $\text{Ti}_3\text{C}_2\text{T}_x$ films. Recently, Diao *et al.* prepared the $\text{Bi}_2\text{Te}_{2.7}\text{Se}_{0.3}/\text{Ti}_3\text{C}_2\text{T}_x$ composite material by simple mixing, vacuum-assisted filtration, and hot pressing [Figure 14C]^[117]. Excellent TE conversion (a ZT value of 1.2 listed in Table 5) and high-performance electromagnetic interference shielding were simultaneously achieved.

TERNARY COMPOSITE TE MATERIALS

Introducing carbon materials with high electrical conductivity into inorganic TE materials fillers with high

Table 5. Room-temperature TE properties of 2D materials

Materials	Preparation method	S ($\mu\text{V/K}$)	σ (S/cm)	PF ($\mu\text{W/mK}^2$)	ZT	Ref.
MoS ₂	Lithium intercalation,	93.5	17.5	13	0.01	[113]
WS ₂	Lithium intercalation	45	30	4.05	-	[114]
WS ₂ /SWCNT	Hydrothermal	43.2	318	61.7	-	[115]
Mo ₂ TiC ₂ T _x	Wet-chemical process	-47.3	1,380	309 (803K)	-	[22]
Ti ₃ C ₂ T _x /SWCNTs/Ti ₃ C ₂ T _x	Lithium intercalation, layer-by-layer stacking	-32.2	750.9	77.9	-	[116]
Bi ₂ Te _{2.7} Se _{0.3} /Ti ₃ C ₂ T _x	Physical mixing, hot pressing	-148	830	1,818	1.2	[117]

TE: Thermoelectric; ZT: thermoelectric figure of merit; PF: PEDOT:PSS-functionalized; SWCNTs: single-walled carbon nanotubes.

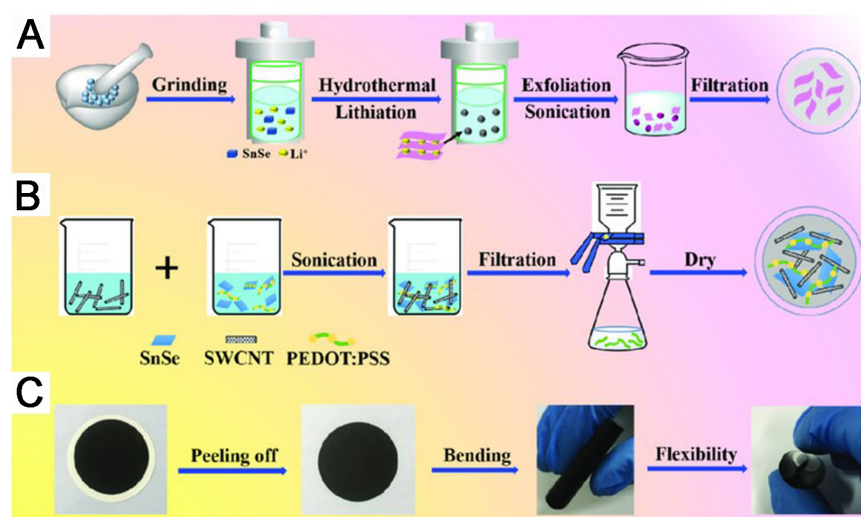


Figure 15. (A) Schematic illustrations for exfoliation of SnSe particles into nanosheets; (B) Fabrication of flexible SWCNT/SnSe/PEDOT:PSS nanocomposite films; (C) Digital photos for fabrication of the free-standing, flexible SWCNT/SnSe/PEDOT:PSS composite films. Reproduced with permission from Ref^[118]. Copyright © 2020. John Wiley and Sons. PEDOT:PSS: Poly(3,4-ethylenedioxythiophene):poly(4-styrenesulfonic acid); SWCNT: single-walled carbon nanotube.

Seebeck coefficients and combining a conducting polymer matrix with low thermal conductivity to prepare ternary composites shall be an effective strategy to achieve excellent TE properties. In such cases, the interfacial contact and interaction between components will directly affect the film formation and properties. The direct vacuum filtration method has been proven to be a good choice. By vacuum filtration, Liu *et al.* prepared flexible SWCNT/SnSe/PEDOT:PSS nanocomposite films on a nylon membrane [Figure 15A-C]^[118]. At 380 K, an optimized power factor of 109.9 $\mu\text{W/mK}^2$ was obtained. The films showed excellent flexibility as their electrical conductivity decreased by 1% after 1000 bending cycles. A flexible TEG is assembled on a polyimide substrate of 8-unit free-standing composite film strips. It generated an open-circuit voltage of 20.6 mV and a maximum output power of 1.16 μW at a temperature gradient of 74.4 K. Other materials with enhanced TE performance have been prepared using similar methods, such as SWCNT/PEDOT:PSS/Te (104 $\mu\text{W/mK}^2$ ^[119]), MWCNT/PEDOT:PSS/Se (73.94 $\mu\text{W/mK}^2$ ^[120]), and MWCNTs/PEDOT:PSS/SnSe (166.5 $\mu\text{W/mK}^2$ ^[121]).

As mentioned above, Ag₂Se is a particularly excellent inorganic TE material. To further improve the TE performance of Ag₂Se, Lu *et al.* have conducted a series of studies on Ag₂Se-based ternary composite materials by vacuum filtration. By adjusting the molar ratio of Cu²⁺:Ag⁺:Se²⁻ in the precursor, they prepared

n-type Ag₂Se/Ag/CuAgSe ternary films with a recorded power factor of 1,593.9 $\mu\text{W}/\text{mK}^2$ ^[122]. The bending test shows that the hybrid film has excellent flexibility, and the power factor only decreases by 10% after bending 1,000 times along the rod with a radius of 4 mm. Optimized carrier transport and the interfacial energy filtering effect of the composite contribute to the ultrahigh power factor. They also prepared PEDOT/Ag₂Se/CuAgSe (1,603 $\mu\text{W}/\text{mK}^2$ ^[123]), Ag₂Se/Ag/PEDOT (1,442 $\mu\text{W}/\text{mK}^2$ ^[124]), Ag₂Se/Se/Polypyrrole (2,240 $\mu\text{W}/\text{mK}^2$ ^[125]) composite films for flexible TEGs. These results are several orders of magnitudes higher than those of Ag₂Se-based composite films prepared from other methods, such as Ag₂Se NW/PEDOT:PSS composite films prepared from a drop-casting method with a maximum room-temperature power factor of 178.59 $\mu\text{W}/\text{mK}^2$ ^[126], and Ag₂Se NW/PEDOT:PSS composite film prepared from a digital light processing-based 3D printing method with a power factor of 81.94 $\mu\text{W}/\text{mK}^2$ ^[127], indicating the significant advantages of vacuum filtration method for the preparation of flexible TE films.

CONCLUSION AND OUTLOOK

Recent years have seen significant progress in using vacuum filtration to advance flexible TE films scientifically and technologically. The current review article highlights the construction of conducting polymer-based, carbon nanoparticle-based, inorganic, two-dimensional materials, and ternary composites, respectively. Despite the recent success in this research area, many critical issues must be addressed.

(1) Currently, the filter membranes used in the filtration method are insulating. On the one hand, they are embedded in the TE film as a flexible skeleton. On the other hand, their insulation affects the overall TE performance, considering that TE materials are the properties of bulk materials. In the future, we could design a filter membrane with high conductivity to provide electrical conductivity further to enhance TE performance while achieving flexible support. Even once the organic TE filter membrane is developed, the composite TE film can be directly prepared through vacuum filtration.

(2) Although some materials can detangle from the filter to form self-supporting films, this is limited to thick films at the micron scale. Is it possible to transfer nano-thickness films such as PEDOT:PSS from the filter membrane substrate to organic optoelectronic devices in the future? Most PEDOT:PSS hole transport layers in organic optoelectronic devices are prepared by spin coating or drip coating methods, which are still difficult to remove PSS. Since the filtration method we discussed above can effectively filter out much PSS-assisted conduction, it is only a step short of transfer to the actual application in organic photoelectric devices. If a breakthrough is made, there will be excellent prospects.

(3) The future of wearable applications will require flexibility, stretchability, and anti-fatigue stability. TE films prepared based on this method have achieved the goal of flexibility, but there are few studies on stretchability, fatigue stability, *etc.* In the future, improving both the substrate and the material may be possible, such as finding a stretchable substrate or further enhancing the binding force between the substrate and the film. Only in this way can the material prepared by the vacuum filtration method realize the leap from flexibility to stretchability and be closer to practical application.

(4) The integrated use of multifunctional equipment is the future development trend of intelligent equipment. For example, combining TE devices and supercapacitors can enable the integration of functions from power generation to power storage. The combination of TE and electrochromic devices allows the device to achieve the role of color change in the environment without a power supply. Suppose the process of preparing TE flexible films by vacuum filtration can be extended to the preparation process of other functional films. The difficulty and cost of preparing multifunctional integrated devices will be significantly simplified in that case. There have been reports on the preparation of flexible supercapacitor films by the

vacuum filtration method, and we expect that there will be reports on the application of multifunctional integrated devices based on the extraction filtration method shortly.

DECLARATIONS

Authors' contributions

Initiated the idea: Jiang Q, Song H

Conducted the literature review: Jiang Q, Wang C

Outlined the manuscript structure: Song H, Jiang Q

Wrote the manuscript draft: Song H, Jiang Q, Wang C, Liu Q

Designed and formatted the figures: Song H, Wang C, Liu Q

Reviewed and revised the manuscript: Song H, Jiang Q

All authors have read the manuscript and approved the final version.

Availability of data and materials

Not applicable.

Financial support and sponsorship

This work was supported by the Natural Nature Science Foundation of China (52203221); the Natural Science Foundation of Guangdong Province (2022A1515010063); SAFEA: the High-End Foreign Experts Project (G2022163014L); the Science and Technology Bureau Project of Jiaying (Grant No. 2020AY10010), and the Research Training Program for College Students of Jiaying University in 2022 (CD 8517221295).

Conflicts of interest

All authors declared that there are no conflicts of interest.

Ethical approval and consent to participate

Not applicable.

Consent for publication

Not applicable.

Copyright

© The Author(s) 2023.

REFERENCES

1. Gao M, Wang P, Jiang L, et al. Power generation for wearable systems. *Energy Environ Sci* 2021;14:2114-57. [DOI](#)
2. Wang Q, Sun X, Liu C, et al. Current development of stretchable self-powered technology based on nanomaterials toward wearable biosensors in biomedical applications. *Front Bioeng Biotechnol* 2023;11:1164805. [DOI](#) [PubMed](#) [PMC](#)
3. Jia Y, Jiang Q, Sun H, et al. Wearable thermoelectric materials and devices for self-powered electronic systems. *Adv Mater* 2021;33:e2102990. [DOI](#)
4. Hong M, Wang Y, Liu W, et al. Arrays of planar vacancies in superior thermoelectric $\text{Ge}_{1-x}\text{YCd}_x\text{Bi}_y\text{Te}$ with band convergence. *Adv Energy Mater* 2018;8:1801837. [DOI](#)
5. Hong M, Wang Y, Feng T, et al. Strong phonon-phonon interactions securing extraordinary thermoelectric $\text{Ge}_{1-x}\text{Sb}_x\text{Te}$ with Zn-alloying-induced band alignment. *J Am Chem Soc* 2019;141:1742-8. [DOI](#)
6. An CJ, Kang YH, Song H, Jeong Y, Cho SY. Highly integrated and flexible thermoelectric module fabricated by brush-cast doping of a highly aligned carbon nanotube web. *ACS Appl Energy Mater* 2019;2:1093-101. [DOI](#)
7. Vieira EM, Figueira J, Pires AL, et al. Enhanced thermoelectric properties of Sb_2Te_3 and Bi_2Te_3 films for flexible thermal sensors. *J Alloys Compd* 2019;774:1102-16. [DOI](#)
8. Sun T, Peavey JL, David Shelby M, Ferguson S, O'connor BT. Heat shrink formation of a corrugated thin film thermoelectric generator. *Energy Convers Mana* 2015;103:674-80. [DOI](#)
9. Owoyele O, Ferguson S, O'connor BT. Performance analysis of a thermoelectric cooler with a corrugated architecture. *Appl Energy*

- 2015;147:184-91. DOI
10. Song H, Meng Q, Lu Y, Cai K. Progress on PEDOT:PSS/Nanocrystal thermoelectric composites. *Adv Electron Mater* 2019;5:1800822. DOI
 11. Wang Y, Yang L, Shi XL, et al. Flexible thermoelectric materials and generators: challenges and innovations. *Adv Mater* 2019;31:e1807916. DOI
 12. Du Y, Xu J, Paul B, Eklund P. Flexible thermoelectric materials and devices. *Appl Mater Today* 2018;12:366-88. DOI
 13. Zhang L, Shi X, Yang Y, Chen Z. Flexible thermoelectric materials and devices: from materials to applications. *Mater Today* 2021;46:62-108. DOI
 14. Yang Q, Yang S, Qiu P, et al. Flexible thermoelectrics based on ductile semiconductors. *Science* 2022;377:854-8. DOI
 15. Shi X, Chen H, Hao F, et al. Room-temperature ductile inorganic semiconductor. *Nat Mater* 2018;17:421-6. DOI
 16. Hou C, Zhu M. Semiconductors flex thermoelectric power. *Science* 2022;377:815-6. DOI PubMed
 17. Fan Z, Du D, Guan X, Ouyang J. Polymer films with ultrahigh thermoelectric properties arising from significant seebeck coefficient enhancement by ion accumulation on surface. *Nano Energy* 2018;51:481-8. DOI
 18. Wang L, Zhang Z, Liu Y, et al. Exceptional thermoelectric properties of flexible organic-inorganic hybrids with monodispersed and periodic nanophase. *Nat Commun* 2018;9:3817. DOI PubMed PMC
 19. Kim D, Park Y, Ju D, Lee G, Kwon W, Cho K. Energy-filtered acceleration of charge-carrier transport in organic thermoelectric nanocomposites. *Chem Mater* 2021;33:4853-62. DOI
 20. Bubnova O, Khan ZU, Malti A, et al. Optimization of the thermoelectric figure of merit in the conducting polymer poly(3,4-ethylenedioxythiophene). *Nat Mater* 2011;10:429-33. DOI
 21. Jin Q, Jiang S, Zhao Y, et al. Flexible layer-structured Bi₂Te₃ thermoelectric on a carbon nanotube scaffold. *Nat Mater* 2019;18:62-8. DOI PubMed
 22. Kim H, Anasori B, Gogotsi Y, Alshareef HN. Thermoelectric properties of two-dimensional molybdenum-based MXenes. *Chem Mater* 2017;29:6472-9. DOI
 23. Mengistie DA, Chen CH, Boopathi KM, Pranoto FW, Li LJ, Chu CW. Enhanced thermoelectric performance of PEDOT:PSS flexible bulky papers by treatment with secondary dopants. *ACS Appl Mater Interfaces* 2015;7:94-100. DOI PubMed
 24. Xiang J, Drzal LT. Templated growth of polyaniline on exfoliated graphene nanoplatelets (GNP) and its thermoelectric properties. *Polymer* 2012;53:4202-10. DOI
 25. Chelawat H, Vaddiraju S, Gleason K. Conformal, conducting poly(3,4-ethylenedioxythiophene) thin films deposited using bromine as the oxidant in a completely dry oxidative chemical vapor deposition process. *Chem Mater* 2010;22:2864-8. DOI
 26. Lee S, Gleason KK. Enhanced optical property with tunable band gap of cross-linked PEDOT copolymers via oxidative chemical vapor deposition. *Adv Funct Mater* 2015;25:85-93. DOI
 27. Hsin C, Huang C, Wu M, Cheng S, Pan R. Synthesis and thermoelectric properties of indium telluride nanowires. *Mater Res Bull* 2019;112:61-5. DOI
 28. Pang J, Zhang X, Shen L, Xu J, Nie Y, Xiang G. Synthesis and thermoelectric properties of Bi-doped SnSe thin films*. *Chin Phys B* 2021;30:116302. DOI
 29. Varghese T, Dun C, Kempf N, et al. Flexible thermoelectric devices of ultrahigh power factor by scalable printing and interface engineering. *Adv Funct Mater* 2020;30:1905796. DOI
 30. Zeng M, Zavanelli D, Chen J, et al. Printing thermoelectric inks toward next-generation energy and thermal devices. *Chem Soc Rev* 2022;51:485-512. DOI
 31. Kim F, Kwon B, Eom Y, et al. 3D printing of shape-conformable thermoelectric materials using all-inorganic Bi₂Te₃-based inks. *Nat Energy* 2018;3:301-9. DOI
 32. Hong CT, Lee W, Kang YH, et al. Effective doping by spin-coating and enhanced thermoelectric power factors in SWCNT/P3HT hybrid films. *J Mater Chem A* 2015;3:12314-9. DOI
 33. Choi DY, Kang HW, Sung HJ, Kim SS. Annealing-free, flexible silver nanowire-polymer composite electrodes via a continuous two-step spray-coating method. *Nanoscale* 2013;5:977-83. DOI
 34. Zhao X, Mai Y, Luo H, et al. Nano-MoS₂/poly(3,4-ethylenedioxythiophene): poly(styrenesulfonate) composite prepared by a facial dip-coating process for Li-ion battery anode. *Appl Surf Sci* 2014;288:736-41. DOI
 35. Lee SH, Park H, Son W, Choi HH, Kim JH. Novel solution-processable, dedoped semiconductors for application in thermoelectric devices. *J Mater Chem A* 2014;2:13380-7. DOI
 36. Xiong J, Jiang F, Zhou W, Liu C, Xu J. Highly electrical and thermoelectric properties of a PEDOT:PSS thin-film via direct dilution-filtration. *RSC Adv* 2015;5:60708-12. DOI
 37. Song H, Yao Y, Tang C, et al. Tunable thermoelectric properties of free-standing PEDOT nanofiber film through adjusting its nanostructure. *Synth Met* 2021;275:116742. DOI
 38. Ni D, Song H, Chen Y, Cai K. Free-standing highly conducting PEDOT films for flexible thermoelectric generator. *Energy* 2019;170:53-61. DOI
 39. Xu S, Shi X, Dargusch M, Di C, Zou J, Chen Z. Conducting polymer-based flexible thermoelectric materials and devices: from mechanisms to applications. *Prog Mater Sci* 2021;121:100840. DOI
 40. Li M, Bai Z, Chen X, et al. Thermoelectric transport in conductive poly(3,4-ethylenedioxythiophene). *Chin Phys B* 2022;31:027201. DOI

41. Song H, Cai K. Preparation and properties of PEDOT:PSS/Te nanorod composite films for flexible thermoelectric power generator. *Energy* 2017;125:519-25. [DOI](#)
42. Meng Q, Song H, Du Y, Ding Y, Cai K. Facile preparation of poly(3,4-ethylenedioxythiophene): poly(styrenesulfonate)/Ag₂Te nanorod composite films for flexible thermoelectric generator. *J Materiomics* 2021;7:302-9. [DOI](#)
43. Lu Y, Ding Y, Qiu Y, et al. Good performance and flexible PEDOT:PSS/Cu₂Se nanowire thermoelectric composite films. *ACS Appl Mater Interfaces* 2019;11:12819-29. [DOI](#) [PubMed](#)
44. Lu Y, Li X, Cai K, et al. Enhanced-performance PEDOT:PSS/Cu₂Se-based composite films for wearable thermoelectric power generators. *ACS Appl Mater Interfaces* 2021;13:631-8. [DOI](#) [PubMed](#)
45. Du Y, Liu X, Xu J, Shen SZ. Flexible Bi-Te-based alloy nanosheet/PEDOT:PSS thermoelectric power generators. *Mater Chem Front* 2019;3:1328-34. [DOI](#)
46. Liu D, Yan Z, Zhao Y, et al. Facile self-supporting and flexible Cu₂S/PEDOT:PSS composite thermoelectric film with high thermoelectric properties for body energy harvesting. *Results Phys* 2021;31:105061. [DOI](#)
47. Yan Z, Zhao Y, Liu D, et al. Thermoelectric properties of flexible PEDOT:PSS-based films tuned by SnSe via the vacuum filtration method. *RSC Adv* 2020;10:43840-6. [DOI](#) [PubMed](#) [PMC](#)
48. Jiang F, Xiong J, Zhou W, et al. Use of organic solvent-assisted exfoliated MoS₂ for optimizing the thermoelectric performance of flexible PEDOT:PSS thin films. *J Mater Chem A* 2016;4:5265-73. [DOI](#)
49. Wang X, Meng F, Wang T, et al. High performance of PEDOT:PSS/SiC-NWs hybrid thermoelectric thin film for energy harvesting. *J Alloys Compd* 2018;734:121-9. [DOI](#)
50. Liu E, Liu C, Zhu Z, et al. Preparation of poly(3,4-ethylenedioxythiophene):poly(4-styrenesulfonate)/silicon dioxide nanoparticles composite films with large thermoelectric power factor. *J Compos Mater* 2018;52:621-7. [DOI](#)
51. Tian Z, Liu H, Wang N, Liu Y, Zhang X. Facile preparation and thermoelectric properties of PEDOT nanowires/Bi₂Te₃ nanocomposites. *J Mater Sci Mater Electron* 2018;29:17367-73. [DOI](#)
52. Liu H, Liu P, Zhang M, et al. Properties of PEDOT nanowire/Te nanowire nanocomposites and fabrication of a flexible thermoelectric generator. *RSC Adv* 2020;10:33965-71. [DOI](#) [PubMed](#) [PMC](#)
53. Xiong J, Wang L, Xu J, et al. Thermoelectric performance of PEDOT:PSS/Bi₂Te₃-nanowires: a comparison of hybrid types. *J Mater Sci Mater Electron* 2016;27:1769-76. [DOI](#)
54. Wu Q, Zha K, Zhang J, Zhang J, Hai J, Lu Z. SnS/PEDOT:PSS composite films with enhanced surface conductivities induced by solution post-treatment and their application in flexible thermoelectric. *Org Electron* 2023;118:106799. [DOI](#)
55. Li H, Liang Y, Liu S, Qiao F, Li P, He C. Modulating carrier transport for the enhanced thermoelectric performance of carbon nanotubes/polyaniline composites. *Org Electron* 2019;69:62-8. [DOI](#)
56. Wang L, Yao Q, Bi H, Huang F, Wang Q, Chen L. PANI/graphene nanocomposite films with high thermoelectric properties by enhanced molecular ordering. *J Mater Chem A* 2015;3:7086-92. [DOI](#)
57. Hsieh YY, Zhang Y, Zhang L, et al. High thermoelectric power-factor composites based on flexible three-dimensional graphene and polyaniline. *Nanoscale* 2019;11:6552-60. [DOI](#)
58. Xiong J, Jiang F, Shi H, et al. Liquid exfoliated graphene as dopant for improving the thermoelectric power factor of conductive PEDOT:PSS nanofilm with hydrazine treatment. *ACS Appl Mater Interfaces* 2015;7:14917-25. [DOI](#)
59. Jiang Q, Lan X, Liu C, et al. High-performance hybrid organic thermoelectric SWNTs/PEDOT:PSS thin-films for energy harvesting. *Mater Chem Front* 2018;2:679-85. [DOI](#)
60. Zhang Z, Chen G, Wang H, Li X. Template-directed in situ polymerization preparation of nanocomposites of PEDOT:PSS-coated multi-walled carbon nanotubes with enhanced thermoelectric property. *Chem Asian J* 2015;10:149-53. [DOI](#)
61. Song H, Liu C, Xu J, Jiang Q, Shi H. Fabrication of a layered nanostructure PEDOT:PSS/SWCNTs composite and its thermoelectric performance. *RSC Adv* 2013;3:22065-71. [DOI](#)
62. Liu X, Du Y, Meng Q, Shen SZ, Xu J. Flexible thermoelectric power generators fabricated using graphene/PEDOT:PSS nanocomposite films. *J Mater Sci Mater Electron* 2019;30:20369-75. [DOI](#)
63. Du Y, Shi Y, Meng Q, Shen SZ. Preparation and thermoelectric properties of flexible SWCNT/PEDOT:PSS composite film. *Synth Met* 2020;261:116318. [DOI](#)
64. Deng W, Deng L, Li Z, Zhang Y, Chen G. Synergistically boosting thermoelectric performance of PEDOT:PSS/SWCNT composites via the ion-exchange effect and promoting SWCNT dispersion by the ionic liquid. *ACS Appl Mater Interfaces* 2021;13:12131-40. [DOI](#) [PubMed](#)
65. Huang J, Liu X, Du Y. Fabrication of free-standing flexible and highly efficient carbon nanotube film/PEDOT: PSS thermoelectric composites. *J Materiomics* 2022;8:1213-7. [DOI](#)
66. Wang P, Liao Y, Lai Y, et al. Conversion of pristine and p-doped sulfuric-acid-treated single-walled carbon nanotubes to n-type materials by a facile hydrazine vapor exposure process. *Mater Chem Phys* 2012;134:325-32. [DOI](#)
67. Wang H, Hsu JH, Yi SI, et al. Thermally driven large N-type voltage responses from hybrids of carbon nanotubes and poly(3,4-ethylenedioxythiophene) with tetrakis(dimethylamino)ethylene. *Adv Mater* 2015;27:6855-61. [DOI](#)
68. Song H, Qiu Y, Wang Y, et al. Polymer/carbon nanotube composite materials for flexible thermoelectric power generator. *Compos Sci Technol* 2017;153:71-83. [DOI](#)
69. Liang L, Gao C, Chen G, Guo C. Large-area, stretchable, super flexible and mechanically stable thermoelectric films of polymer/carbon nanotube composites. *J Mater Chem C* 2016;4:526-32. [DOI](#)

70. Liang L, Chen G, Guo C. Enhanced thermoelectric performance by self-assembled layered morphology of polypyrrole nanowire/single-walled carbon nanotube composites. *Compos Sci Technol* 2016;129:130-6. DOI
71. Liang L, Wang X, Wang M, Liu Z, Chen G, Sun G. Flexible poly(3,4-ethylenedioxythiophene)-tosylate/SWCNT composite films with ultrahigh electrical conductivity for thermoelectric energy harvesting. *Compos Commun* 2021;25:100701. DOI
72. Zhang L, Harima Y, Imae I. Highly improved thermoelectric performances of PEDOT:PSS/SWCNT composites by solvent treatment. *Org Electron* 2017;51:304-7. DOI
73. Bark H, Lee W, Lee H. Enhanced thermoelectric performance of CNT thin film p/n junctions doped with N-containing organic molecules. *Macromol Res* 2015;23:795-801. DOI
74. Kim J, Kwon OH, Kang YH, Jang K, Cho SY, Yoo Y. A facile preparation route of n-type carbon buckypaper and its enhanced thermoelectric performance. *Compos Sci Technol* 2017;153:32-9. DOI
75. Chortos A, Pochorovski I, Lin P, et al. Universal selective dispersion of semiconducting carbon nanotubes from commercial sources using a supramolecular polymer. *ACS Nano* 2017;11:5660-9. DOI
76. Shimizu S, Iizuka T, Kanahashi K, et al. Thermoelectric detection of multi-subband density of states in semiconducting and metallic single-walled carbon nanotubes. *Small* 2016;12:3388-92. DOI
77. Avery AD, Zhou BH, Lee J, et al. Tailored semiconducting carbon nanotube networks with enhanced thermoelectric properties. *Nat Energy* 2016;1:16033. DOI
78. Wang L, Yao Q, Qu S, Shi W, Chen L. Influence of electronic type of SWNTs on the thermoelectric properties of SWNTs/PANI composite films. *Org Electron* 2016;39:146-52. DOI
79. Tambasov IA, Voronin AS, Evsevskaya NP, et al. Thermoelectric properties of low-cost transparent single wall carbon nanotube thin films obtained by vacuum filtration. *Physica E Low Dimens Syst Nanostruct* 2019;114:113619. DOI
80. Wu D, Huang C. High cross-plane thermoelectric performance of carbon nanotube sponge films. *Int J Energy Res* 2020;44:2332-6. DOI
81. Gao W, Komatsu N, Taylor LW, et al. Macroscopically aligned carbon nanotubes for flexible and high-temperature electronics, optoelectronics, and thermoelectrics. *J Phys D Appl Phys* 2020;53:063001. DOI
82. Matsumoto M, Yamaguchi R, Shima K, et al. Control of anisotropic conduction of carbon nanotube sheets and their use as planar-type thermoelectric conversion materials. *Sci Technol Adv Mater* 2021;22:272-9. DOI PubMed PMC
83. Gee C, Tseng C, Wu F, et al. Few layer graphene paper from electrochemical process for heat conduction. *Mater Res Innov* 2014;18:208-13. DOI
84. Zhao W, Tan HT, Tan LP, et al. n-Type carbon nanotubes/silver telluride nanohybrid buckypaper with a high-thermoelectric figure of merit. *ACS Appl Mater Interfaces* 2014;6:4940-6. DOI
85. Bark H, Kim J, Kim H, Yim J, Lee H. Effect of multiwalled carbon nanotubes on the thermoelectric properties of a bismuth telluride matrix. *Curr Appl Phys* 2013;13:S111-4. DOI
86. Chen X, Feng L, Yu P, et al. Flexible thermoelectric films based on Bi₂Te₃ nanosheets and carbon nanotube network with high n-type performance. *ACS Appl Mater Interfaces* 2021;13:5451-9. DOI PubMed
87. Fan J, Huang X, Liu F, Deng L, Chen G. Feasibility of using chemically exfoliated SnSe nanobelts in constructing flexible SWCNTs-based composite films for high-performance thermoelectric applications. *Compos Commun* 2021;24:100612. DOI
88. Gao J, Liu C, Miao L, Wang X, Peng Y, Chen Y. Enhanced power factor in flexible reduced graphene oxide/nanowires hybrid films for thermoelectrics. *RSC Adv* 2016;6:31580-7. DOI
89. Xiao Z, Du Y, Meng Q, Wang L. Thermoelectric characteristics of flexible reduced graphene oxide/silver selenide nanowire composites prepared by a facile vacuum filtration process. *Chinese Phys B* 2022;31:028103. DOI
90. Chen Z, Cui Y, Liang L, et al. Flexible film and thermoelectric device of single-walled carbon nanotube@conductive metal-organic framework composite. *Mater Today Nano* 2022;20:100276. DOI
91. Yang S, Qiu P, Chen L, Shi X. Recent Developments in Flexible Thermoelectric Devices. *Small Sci* 2021;1:2100005. DOI
92. Ding Y, Qiu Y, Cai K, et al. High performance n-type Ag₂Se film on nylon membrane for flexible thermoelectric power generator. *Nat Commun* 2019;10:841. DOI PubMed PMC
93. Drymiotis F, Day TW, Brown DR, Heinz NA, Jeffrey Snyder G. Enhanced thermoelectric performance in the very low thermal conductivity Ag₂Se_{0.5}Te_{0.5}. *Appl Phys Lett* 2013;103:143906. DOI
94. Lu Y, Liu Y, Li Y, Cai K. The influence of Ga doping on preparation and thermoelectric properties of flexible Ag₂Se films. *Compos Commun* 2021;27:100895. DOI
95. Wu M, Cai K, Li X, et al. Ultraflexible and high-thermoelectric-performance sulfur-doped Ag₂Se film on nylon for power generators. *ACS Appl Mater Interfaces* 2022;14:4307-15. DOI PubMed
96. Jiang C, Ding Y, Cai K, et al. Ultrahigh performance of n-type Ag₂Se films for flexible thermoelectric power generators. *ACS Appl Mater Interfaces* 2020;12:9646-55. DOI PubMed
97. Jiang C, Wei P, Ding Y, et al. Ultrahigh performance polyvinylpyrrolidone/Ag₂Se composite thermoelectric film for flexible energy harvesting. *Nano Energy* 2021;80:105488. DOI
98. Liu Y, Lu Y, Wang Z, et al. High performance Ag₂Se films by a one-pot method for a flexible thermoelectric generator. *J Mater Chem A* 2022;10:25644-51. DOI
99. Gao Q, Wang W, Lu Y, et al. High Power Factor Ag/Ag₂Se composite films for flexible thermoelectric generators. *ACS Appl Mater Interfaces* 2021;13:14327-33. DOI

100. Li X, Lu Y, Cai K, et al. Exceptional power factor of flexible Ag/Ag₂Se thermoelectric composite films. *J Chem Eng* 2022;434:134739. DOI
101. Wu W, Liang Z, Jia M, et al. High power factor of Ag₂Se/Ag/Nylon composite films for wearable thermoelectric devices. *Nanomaterials* 2022;12:4238. DOI PubMed PMC
102. Palaporn D, Mongkolthananuk W, Tanusilp S, Kurosaki K, Pinitsoontorn S. A simple method for fabricating flexible thermoelectric nanocomposites based on bacterial cellulose nanofiber and Ag₂Se. *Appl Phys Lett* 2022;120:073901. DOI
103. Zhou H, Zhang Z, Sun C, Deng H, Fu Q. Biomimetic approach to facilitate the high filler content in free-standing and flexible thermoelectric polymer composite films based on PVDF and Ag₂Se nanowires. *ACS Appl Mater Interfaces* 2020;12:51506-16. DOI PubMed
104. Zhang Y, Zhao Y, Guo R, Zhang Z, Liu D, Xue C. Effect of L-ascorbic acid solution concentration on the thermoelectric properties of silver selenide flexible films prepared by vacuum-assisted filtration. *Nanomaterials* 2022;12:624. DOI PubMed PMC
105. Zhou C, Dun C, Wang Q, et al. Nanowires as building blocks to fabricate flexible thermoelectric fabric: the case of copper telluride nanowires. *ACS Appl Mater Interfaces* 2015;7:21015-20. DOI
106. Pammi SVN, Jella V, Choi J, Yoon S. Enhanced thermoelectric properties of flexible Cu_{2-x}Se (x ≥ 0.25) NW/polyvinylidene fluoride composite films fabricated via simple mechanical pressing†. *J Mater Chem C* 2017;5:763-9. DOI
107. Han X, Lu Y, Liu Y, et al. CuI/Nylon membrane hybrid film with large seebeck effect. *Chin Phys Lett* 2021;38:126701. DOI
108. Zeng X, Ren L, Xie J, et al. Room-temperature welding of silver telluride nanowires for high-performance thermoelectric film. *ACS Appl Mater Interfaces* 2019;11:37892-900. DOI
109. Yu P, Feng L, Tang W, et al. Robust, flexible thermoelectric film for energy harvesting by a simple and eco-friendly method. *ACS Appl Mater Interfaces* 2023;15:13144-54. DOI
110. Zhao X, Zhao C, Jiang Y, et al. Flexible cellulose nanofiber/Bi₂Te₃ composite film for wearable thermoelectric devices. *J Power Sources* 2020;479:229044. DOI
111. Dong Z, Liu H, Yang X, et al. Facile fabrication of paper-based flexible thermoelectric generator. *npj Flex Electron* 2021;5:6. DOI
112. Wu M, Li J, Liu Y, et al. High thermoelectric performance and ultrahigh flexibility Ag₂S_{1-x}Se_x film on a nylon membrane. *ACS Appl Mater Interfaces* 2023;15:8415-23. DOI PubMed
113. Wang T, Liu C, Xu J, et al. Thermoelectric performance of restacked MoS₂ nanosheets thin-film. *Nanotechnology* 2016;27:285703. DOI PubMed
114. Piao M, Chu J, Wang X, et al. Hydrothermal synthesis of stable metallic 1T phase WS₂ nanosheets for thermoelectric application. *Nanotechnology* 2018;29:025705. DOI PubMed
115. Piao M, Li C, Joo M, et al. Hydrothermal synthesis of stable 1T-WS₂ and single-walled carbon nanotube hybrid flexible thin films with enhanced thermoelectric performance. *Energy Technol* 2018;6:1921-8. DOI
116. Ding W, Liu P, Bai Z, et al. Constructing layered MXene/CNTs composite film with 2D-3D sandwich structure for high thermoelectric performance. *Adv Mater Interfaces* 2020;7:2001340. DOI
117. Diao J, Yuan J, Cai Z, et al. High-performance electromagnetic interference shielding and thermoelectric conversion derived from multifunctional Bi₂Te_{2.7}Se_{0.3}/MXene composites. *Carbon* 2022;196:243-52. DOI
118. Liu X, Du Y, Meng Q, et al. Free-standing single-walled carbon nanotube/SnSe nanosheet/poly(3,4-ethylenedioxythiophene):poly(4-styrenesulfonate) nanocomposite films for flexible thermoelectric power generators. *Adv Eng Mater* 2020;22:2000605. DOI
119. Meng Q, Cai K, Du Y, Chen L. Preparation and thermoelectric properties of SWCNT/PEDOT:PSS coated tellurium nanorod composite films. *J Alloys Compd* 2019;778:163-9. DOI
120. Park D, Kim M, Kim J. Facile fabrication of poly(3,4-ethylenedioxythiophene):poly(styrenesulfonate)-coated selenium nanowire/carbon nanotube composite films for flexible thermoelectric applications. *Dalton Trans* 2021;50:12424-9. DOI
121. Liu D, Yan Z, Zhao Y, et al. Facile MWCNTs-SnSe/PEDOT:PSS ternary composite flexible thermoelectric films optimized by cold-pressing. *J Mater Res Technol* 2021;15:4452-60. DOI
122. Lu Y, Qiu Y, Cai K, et al. Ultrahigh power factor and flexible silver selenide-based composite film for thermoelectric devices. *Energy Environ Sci* 2020;13:1240-9. DOI
123. Lu Y, Qiu Y, Cai K, et al. Ultrahigh performance PEDOT/Ag₂Se/CuAgSe composite film for wearable thermoelectric power generators. *Mater Today Phys* 2020;14:100223. DOI
124. Wang Z, Gao Q, Wang W, et al. High performance Ag₂Se/Ag/PEDOT composite films for wearable thermoelectric power generators. *Mater Today Phys* 2021;21:100553. DOI
125. Li Y, Lou Q, Yang J, et al. Exceptionally high power factor Ag₂Se/Se/polypyrrole composite films for flexible thermoelectric generators. *Adv Funct Mater* 2022;32:2106902. DOI
126. Park D, Kim M, Kim J. Fabrication of PEDOT:PSS/Ag₂Se nanowires for polymer-based thermoelectric applications. *Polymers* 2020;12:2932. DOI PubMed PMC
127. Park D, Lee S, Kim J. Thermoelectric and mechanical properties of PEDOT:PSS-coated Ag₂Se nanowire composite fabricated via digital light processing based 3D printing. *Compos Commun* 2022;30:101084. DOI